FATIGUE TESTS OF SMALL-SIZE TUBULAR T-JOINTS

By Y. Kurobane, M. Natarajan, and A. A. Toprac

FATIGUE TESTS ON SMALL-SIZE TUBULAR T-JOINTS

KEY WORDS: fatigue; fatigue strength; static strength; steel; structural engineering; tube, tubular joints

ABSTRACT: Results on the fatigue tests of tubular T-joints are presented. The specimens consisted of about one hundred small-size T-joints. S-N curves were established for initiation of crack and for complete failure of the joints. The parameters which influence the fatigue strength of tubular T-joints are discussed.

FATIGUE TESTS OF SMALL-SIZE TUBULAR T-JOINTS

By Y.Kurobane[1], M.Natarajan[2], and A.A.Toprac[3]

INTRODUCTION

One of the factors that cause the failure of joints in offshore drilling platforms is fatigue. Most tubular joints are, in general, subjected to large local stresses in the tube walls around the welded portions. Invariably cracks were observed at these locations. Several studies of tubular joints have been carried out under static loads. Studies of the fatigue behavior of tubular joints are important because together with the studies under static loading will enable engineers to formulate design procedures for offshore structures subjected to both static and repetitive types of loads.

Test results of small-size tubular T-joints subjected to repetitive loading are discussed in this paper. The objective of this investigation was to study the influence of stress concentration due to geometry on the fatique behavior of T-joints. A T-joint consists of a larger tube, the chord, and a smaller tube, the brace, welded at right angles to the chord axis. The T-joints were selected because of their simple configuration. Further, the

---

[1]Associate Professor, Kumamoto University, Kumamoto, Japan

[2]Research Engineer, Department of Civil Engineering, University of Texas at Austin, Austin, Texas

[3]Professor of Civil Engineering, University of Texas at Austin, Austin, Texas

chord walls of T-joints have to sustain severe stress concentration which is typical in the tubular joints.

Offshore structures are subjected to maximum loading by repetitive wave forces during a storm. Thus, the number of cycles of peak load which the structure has to withstand in its service period is limited. Consequently, in this investigation the fatigue behavior in the lower range of cycles (about 10^5 cycles) is studied.

SPECIMENS AND MATERIAL PROPERTIES

The specimens were divided into five types, A through E, as shown in Fig. 1. All the specimens consisted of 2 1/4" diameter chord members. One or more of the following parameters were varied in grouping the specimens:

1. The ratio of chord length to mean chord radius, α.
2. The ratio of mean radii of brace and chord, β.
3. The ratio of mean chord radius to chord thickness, γ.
4. The ratio of the brace thickness to the chord thickness, τ.

For all the specimens, brace and chord members were cold formed welded tubes. The mechanical properties of the material of the tubes as determined by tensile coupons are given in Table 1. The material specification of the tubes of diameter less than 2 1/4" is not known.

Gas tungsten-arc, and electric arc welding with coated electrodes were used to fabricate the specimens. The gas

tungsten-arc welding process produced welds with better penetration and smaller size than the regular arc welding. The edges of braces were beveled prior to welding. For each specimen the weld sizes, S_c and S_ℓ, were measured and are shown in Fig. 1.

TEST PROGRAM

Type A, C, D, and E specimens were subjected to fully reversed loads. That is, the stress ratio R (minimum stress, S_{min}/ maximum stress, S_{max}) was -1.0. Type B specimens were subjected to completely reversed stress and also to other patterns of stress cycles with R = 0, 0.16 and 0.50. In all the tests, except for Type B specimens with R = -1.0, stress levels were selected such that fracture would occur around 10^5 cycles. Static tests to fracture were carried out only for two Type B specimens which are designated as BP in Table 2.

The stresses S_{max} and S_{min}, to compute R, are the average stresses acting on the shear area of the chord. The shear area is defined as the product of wall thickness of the chord and length of the intersecting line formed by the chord and the brace surfaces. For Type A specimens (see Fig. 1) the circumference of the brace was taken as the length of the intersecting line. For the rest of the specimens the length of the intersecting line was obtained by approximate equations given in B.S.449 (3)[4]. The computed shear areas are given in Table 1.

---

[4]Numerals in parentheses refer to corresponding items in Appendix I - References.

The fatigue loads were applied by a Sonntag machine which produces a sinusoidal force of frequency same as the natural frequency of the spring connecting the vibrating and stationary cages of the machine. The test setup is shown in Fig. 2.

INSTRUMENTATION AND CRACK DETECTION

The formation of cracks were observed at first by a magnifying lens for a few specimens. Since it was difficult to detect crack initiation by this method, kerosene was used as a detector. The chord of the specimens was filled with kerosene prior to the application of the load. Leakage of kerosene during the test through the chord wall was considered as indication of crack initiation. The number of cycles corresponding to crack initiation and to complete failure (cycles at which the brace separates from the chord) are given in Table 2.

For some of the specimens (for example, Specimen B-1) fatigue testing was stopped after a certain number of load cycles to perform a static test. Dial gages and strain gages were employed during such tests to measure deformations and strains.

STRESS CONCENTRATION AND FATIGUE CRACKS

In previous investigations (1,2) on the static behavior of the tubular joints, discussions on high localized stresses in the chord, when the brace is subjected to axial forces, are presented. These high stresses at the points of stress concentration (Fig. 3) were found mainly due to bending stresses in the chord walls in

the circumferential direction (1,2). The stress concentration factor which decreased as β and γ were decreased was found to be even greater than 30 for certain types of specimens.

The fatigue cracks initiated, in most of the specimens tested, at the points of stress concentration. Only in a few of the specimens, as indicated in Table 2, the cracks initiated elsewhere. In general, there exists two points of peak stress concentration in a T-joint, 180 degrees apart (see Fig. 3). The first crack was found at either one of these points. As the number of cycles increased, the second crack developed at the other point of stress concentration.

In general, the cracks propagated along the toe of the weld. When the first and second cracks extended to a certain length, the remaining portion of the chord wall at the crown was suddenly torn resulting to a complete failure. Typical failure mode for Type B specimens is shown in Fig. 4. The surface of the crack at the center section of the chord was smoother than the portions where crack extended. The appearance of chord wall at the crown after the failure of the specimen was similar to a fracture due to a static tensile load. The propagation of the fatigue cracks was rather slow. The number of cycles to detectable crack initiation was about half of that to complete failure (see Table 2).

The stress distribution patterns in the joints changed after the cracks were initiated at the points of stress concentration.

The stresses at the toe of the weld in the circumferential direction seem to vanish once a crack was formed. The gradient of stress near the weld toe becomes less as the number of cycles increases after crack formation. The longitudinal strains in the brace near the brace to chord welds were measured and are shown in Fig. 5. During the preliminary static test, negative values of the longitudinal strains near the crown of the chord were noted. After the formation of the first crack the strain at the point near the crack, however, began to decrease and the strains at the other points began to increase. At that instant the highest strain was observed at the second point of stress concentration, and subsequently the second crack was found at that point. After the formation of the second crack, the strains near the crown of the chord became positive.

The test results indicate that the stress redistribution occurs after the formation of a crack. The portions of the specimens other than those near the crack carry more load.

STATIC FAILURE

The failure pattern of small-size specimens under static loads was quite different from that reported (1,2). The chords sustained large bending deformations. The chord walls located around the weld lines were finally torn in a manner similar to tension failure (Fig. 6). The large-size specimens tested previously (1,2) failed by complete separation at the base metal of the chord. The difference is most likely due to the high ductility (62% elongation on 2" gage) of the material of the small-size specimens. The

average stresses in the shear area of the small-size specimens at ultimate loads were approximately twice as much as those of the large-size specimens (1,2).

FATIGUE STRENGTH

The stress concentration, as mentioned earlier, is the important factor affecting the fatigue strength of tubular T-joints. The stress concentration factor varies with the geometrical parameters, such as the β and γ ratios. To investigate the effects of the β and γ ratios on the fatigue strength of the T-joints, S-N curves were established for each type of specimens.

The relationships of stress amplitude "S_a" in the shear area to the number of cycles "N" for crack initiation and for complete failure are presented on semi-logarithmic coordinates in Figs. 7 through 13. The solid lines drawn in these figures are the S-N curves fitted by the method of least squares, in which the quantity S was assumed to have homogeneous variance for the reversal test results of B specimens (Figs. 8 and 9), while, for the rest of the S-N curves, the quantity log N was assumed to have homogeneous variance. The technique used for this curve fitting is the same as that described by Weibull (4). It is seen from these figures that the test results are scattered considerably. S-N curves for Type B specimens with R = 0.5 and for Type D specimens are not shown since only a few specimens were tested.

It is possible to estimate the fatique strength for each type of specimen from the fitted S-N curves. The fatigue strengths at

10^5 and 2 x 10^5 cycles obtained from the fitted curves are shown in Table 3. Most of the S-N curves cover the above range of cycles. For Type E specimens the S-N curves were extended (Fig. 13) to cover the range of cycles mentioned earlier.

EFFECTS OF β AND γ RATIOS

The stress concentration factor of T-joints varies with β and γ ratios. The stress concentration factor obtained from an empirical equation (1) is given in Table 4 for five types of specimens tested. Table 4 shows that the stress concentration factor was greatest for Type C specimens (β = 0.656) and decreases as β increases.

The relationships between β and the fatigue strength given in Table 3 are illustrated in Fig. 14. The fatique strength is lowest for Type B specimens (β = 0.432). Type A specimens (β = 0.216) had higher fatigue strength. The fatigue strength of Type D specimens (β = 0.885) was not obtained. However, from Table 2 it can be inferred that the fatigue strength of Type D specimens is higher than that of Type C specimens. From the specimens tested, it can be concluded that the fatigue strength takes the lowest value around β = 0.43 since Type C specimens have slightly higher fatigue strength than Type B specimens.

The fatigue strength to β relationships generally agree with the relationships between the stress concentration factor and β due to the fact that the fatique strength should decrease as the stress concentration factor increases. However, it should be noted that the stress concentration factors in Table 4 are approximate. The

experimental equation for the stress concentration factor (1) was based on test results which covered limited ranges of α, β, γ, and τ ratios, and which required an extrapolation to obtain stresses at the toe of the weld of the specimens.

The fatigue strength became higher as γ ratio was decreased. This is seen in Table 3 by comparing Type B specimens ($\gamma = 24$) and Type E specimens ($\gamma = 14$). The stress concentration factor is smaller for Type E specimens than for Type B specimens. This agrees with the fatigue behavior. The modified Goodman diagram shown in Fig. 15 illustrates the fatigue strength of Type B specimens for lives of 10^5 and 2×10^5 cycles.

CONCLUSIONS

In this report the fatigue test results of small-size tubular T-joints are presented. The specimens consisted of about one hundred T-joints of various β and γ ratios subjected to certain patterns of stress cycles ($R = -1.0$, 0.0, 0.16 and 0.5). The following conclusions can be derived based on the test results:

1. The stress concentration is an important factor influencing the fatigue behavior of T-joints. The points of highest stress concentration in the chord walls (Fig. 3) are at the toe of the welds. The fatigue cracks initiated at these points and crack propagation in most of the specimens tested was rather slow along the toe of the weld. This is possibly due to stress

redistribution. The joints survived approximately twice the number of cycles to crack initiation.

2. The fatigue strength expressed in terms of the stress amplitude in the shear area was obtained from the S-N curves of the specimens. The fatigue strength to β relationships were shown in a concave-upward curve having the lowest fatigue strength around $\beta = 0.43$. The variation of the fatigue strength due to β is not very critical from the view point of an actual design. The fatigue strength increased as γ ratio was decreased.

ACKNOWLEDGMENTS

This research work was carried out at the Structures Fatigue Research Laboratory of The University of Texas at Austin, under the supervision of the Subcommittee on Welded Tubular Structures of the Welding Research Council and with funds supplied by the Naval Facilities Engineering Command (Bureau of Yards and Docks).

The authors acknowledge with appreciation the help and interest of Dr. A. Amirikian of the Naval Facilities Engineering Command, and that of Mr. C. F. Larson, Secretary, Welding Research Council. Also, the authors wish to acknowledge the valuable assistance rendered by members of the Subcommittee and its Chairman, Mr. R. R. Graham.

APPENDIX I.- REFERENCES

1. Beale, L. A., and Toprac, A. A., "Research in Tubular Connections: Analysis of T, Y, and K Welded Tubular Connections," Structures Fatigue Research Laboratory Technical Report P 550-9, The University of Texas at Austin, Austin, Texas, April, 1967.

2. Noel, J. S., Beale, L. A., and Toprac, A. A., "An Investigation of Stresses in Welded T-Joints," Structures Fatigue Research Laboratory Technical Report 550-3, The University of Texas at Austin, Austin, Texas, March, 1965.

3. "Specification for the Use of Structural Steel in Buildings, B.S. 449," British Standard Institution, London, 1959, p. 93.

4. "Weibull, W., "Fatigue Testing and Analysis of Results," Pergamon Press, New York, 1961, Section 91.

APPENDIX II - NOTATION

The following symbols are used in this paper:

a	mean chord radius
C	mean brace radius
D	outer diameter of chord
d	outer diameter of brace
L	chord length
N	number of cycles
R	stress ratio, S_{min}/S_{max}
S_a	stress amplitude, $1/2\ (S_{max} - S_{min})$
S_c, S_ℓ	size of welds (see Fig. 1)
S_{max}	maximum stress
S_{min}	minimum stress
T	chord thickness
t	brace thickness
α	ratio of chord length to mean chord radius, L/a
β	ratio of mean radii of brace and chord, C/a
ε	strain
γ	ratio of mean chord radius to chord thickness, a/T
τ	ratio of brace thickness to chord thickness, t/T

FATIGUE TESTS OF TUBULAR T-JOINTS

by

Y. Kurobane,
M. Natarajan
and
A. A. Toprac

This work has been carried out as part of an investigation supervised by the Welding Research Council with funds furnished by The Naval Facilities Engineering Command, U.S. Department of the Navy, Washington, D. C.

November 1967

Structures Fatigue Research Laboratory
University of Texas
Austin, Texas

TABLE OF CONTENTS

ACKNOWLEDGMENT

This research work was carried out at the Structures Fatigue Research Laboratory of the University of Texas at Austin with funds supplied by the Naval Facilities Engineering Command (Bureau of Yards and Docks) whose support is gratefully appreciated.

The authors of this report acknowledge with appreciation the help and interest of Dr. A. Amirikian of the Naval Facilities Engineering Command.

The Subcommittee on Welded Tubular Structures of the Welding Research Council, which guided this project, has the following members: A. Amirikian, J. G. Bouwkamp, G. C. Lee, B. J. DeGeorge, R. R. Graham (Chairman), LaMotte Grover, T. R. Higgins, G. H. Holliday, R. L. Ketter, W. E. Kindel, C. F. Larson (Secretary), A. Lubinski, J. Powers, J. Schneider, A. A. Toprac, and E. I. White.

The authors wish to acknowledge the valuable assistance rendered by members of this Subcommittee. Thanks are due to Mr. K. H. Koopman, Director and C. F. Larson, Secretary, Welding Research Council, for their interest in the project and help.

FATIGUE TESTS OF TUBULAR T-JOINTS

by

Y. Kurobane,[1] M. Natarajan,[2] and A. A. Toprac[3]

1. INTRODUCTION

The failure of joints in the offshore drilling platforms is mainly due to fatigue cracks. Stress concentration due to geometry is a primary factor influencing the fatigue failure of these joints. Most of the joints of tubular members are, in general, subjected to large local bending stresses in the tube walls around the welded portions. Invariably cracks are observed in these portions.

The test results of tubular T-joints subjected to repetitive loading are discussed in this report. The objective of this investigation was to study the influence of geometrical stress concentration on the fatigue behavior of T-joints. A T-joint consists of a larger tube, the chord, and a smaller tube, the brace, welded at right angles to the chord wall. The T-joints were selected because of their simplest configuration. Further, the chord walls of T-joints have to sustain severe stress concentration which is typical in the tubular joints.

Offshore structures are subjected to maximum loading by repetitive wave forces during a storm. Thus, the number of cycles of peak load which the structure has to withstand in its service period is limited. Consequently, in this investigation the fatigue behavior in the lower range of cycles (about 10^5 cycles) is studied. However, further research is necessary to formulate design recommendations for offshore structures.

---

[1]Associate Professor, Kumamoto University, Kumamoto, Japan.

[2]Research Engineer, Department of Civil Engineering, University of Texas at Austin.

[3]Professor of Civil Engineering at The University of Texas at Austin.

2. DESCRIPTION OF TESTS

2.1 Specimens and Material Properties

The specimens were divided into six types, A through F, as shown in Table 1. The configuration of the specimens is shown in Fig. 1. One or more of the following four parameters were varied in grouping the specimens:

1. The ratio of chord length to mean chord radius, α.
2. The ratio of mean radii of brace and chord, β.
3. The ratio of mean chord radius to chord thickness, γ.
4. The ratio of the brace thickness to the chord thickness, τ.

Specimens of type A through E consisted of 2 1/4" diameter chord members. Specimens of type F on the other hand had 8 5/8" diameter chord members. The parameters β and γ of specimens F are almost equal to those of B specimens. Specimens BP (Table 2) used in preliminary tests had the same configuration as specimens B. Cold formed welded tubes were used for specimens A to E. The mechanical properties of the material of the tubes as determined by tensile coupons are given in Table 3. The material specification of the tubes of diameter less than 2 1/4" is not known. The tubes of diameters 8 5/8" and 3 3/4" are of structural grade steel equivalent to A36.

Gas tungsten-arc welding and regular arc welding with the covered electrode were used to fabricate the small-size (A through E) specimens. The gas tungsten-arc welding process produced welds with better penetration and smaller size than the regular arc welding. The edges of braces were beveled prior to welding. For each specimen the weld sizes, S_c and S_L were measured and are given in Table 1.

2.2 Test Program

Specimens A, C, D, and E were subjected to fully reversed loads. That is, the stress ratio R, of minimum stress to maximum stress, was -1.0. Specimens B were subjected not only to fully reversed loads but also to other patterns of stress cycles with R = 0, 0.16 and 0.50. Specimens F had a stress ratio of 0.16. In all the tests of small-size specimens except specimens B with R = -1.0, stress levels were selected such that fracture would occur around 10^5 cycles. Static tests to fracture were carried out only for two B specimens.

The stress given in Table 2 for every specimen is the average stress acting on the shear area of the chord. The shear area is defined as the product of wall thickness of the chord and length of the intersecting line formed by the chord and the brace surfaces. The circumference of the brace was taken as the length of the intersecting line for Type A specimens. The length of the intersecting line was obtained for the rest of the specimens by approximate equations given in B.S. 449.[1] The computed shear areas of the specimens are given in Table 1.

The fatigue loads were applied by a Sonntag fatigue machine for the small-size specimens and by a Riehle-Los hydraulic machine for specimens F. The Sonntag machine produces a sinusoidal force which has the same frequency as the natural frequency of the spring connecting the vibrating and stationary cages of the machine. A complimentary weight was added to the vibrating cage to adjust the natural frequency of the spring to 1800 cpm, which is equal to the rpm of the rotating

eccentric mass attached to the vibrating cage. Figure 2 shows the dynamic load on an aluminum load cell after the calibration of the machine. Test set-up for specimens A through E is shown in Figs. 3 and 4. The repeated tensile load was applied to the braces of specimens F by a cylinder of 24 kips capacity through a loading rig. The frequency of the load was about 150 cpm. The effect of inertia force was taken into consideration in setting the dynamic load on the pulsator. Figures 5 and 6 show the test set-up for specimens F.

2.3 Instrumentation and Crack Detection

At the beginning, the formation of cracks was observed by a magnifying lens. However, for specimens A to E it was difficult to detect crack initiation by this method. Kerosene was therefore used as a detector. The chord of all the specimens was filled with kerosene prior to the application of the load. Leakage of kerosene during the test through the chord wall was considered as indication of crack initiation. For specimens F the fatigue cracks were detected both with a magnifying lens and kerosene. In all three specimens of type F the cracks were first detected by the magnifying glass. Leakage of kerosene followed presumably after the crack propagated through the wall thickness after a small number of additional cycles. Therefore, for all practical purposes kerosene leakage is considered taking place at crack initiation. The number of cycles corresponding to crack initiation and to complete failure* are given in Table 2.

For some of the specimens fatigue testing was stopped after a certain number of load cycles to perform a static test. Deflection dials and strain gages were used during such tests to measure deformations and strains.

*Cycles at which the brace separates from chord.

3. STRESS CONCENTRATION AND FATIGUE CRACKS

3.1 Stress Distribution in Elastic Range

High localized stresses in the chord are produced when the brace is subjected to axial force. The magnitude of these local stresses is far greater than the fiber stresses obtained by assuming the chord as a simple beam subjected to a concentrated load at the center. The local stresses have a steep gradient and become maximum at the toes of the welds. The stress becomes highest at the point in the chord shown in Fig. 7.

Extensive investigation on the stress distribution of T-joints was previously carried out at The University of Texas.[2],[3] Many rosette gages were mounted on T-joint specimens having chord members 8 5/8" to 16" diameter. The stresses at the toes of the welds were estimated by extrapolating the stress distribution curves obtained from strain readings. The numerical analyses of T-joints were made assuming the chords and the braces as thin shells and considering only membrane stresses in the braces. The chord and the brace of a T-joint were assumed to be connected by pins along the intersecting curve.

3.2 Stress Concentration Factor

A greater part of the high stress at the point of stress concentration, according to the investigations mentioned above, is due to the bending stress of the chord walls in the circumferential direction. The stress concentration factor, defined as the ratio of the highest stress to the average stress of the shear area, was found to be even greater

than 30 for certain types of specimens. The stress concentration factor decreased as β and γ were increased.

The measured and calculated circumferential stress distribution on the chord surface of specimen F-2 is shown in Fig. 8. The β-ratio for the theoretical analysis was based on the intersecting line A-A as shown in Fig. 8. The peak stress at the toe of the welds obtained by extrapolating the stresses from measured strains is 57 ksi. This yields a stress concentration factor of 13. The peak stress according to the theoretical analysis is 60 ksi and the corresponding stress concentration factor is 14.

3.3 Fatigue Cracks

The fatigue cracks in most specimens initiated at the points of stress concentration near the toe of the welds at the center section of the chord. Only in a few of the specimens, as indicated in Table 2, the cracks occurred elsewhere. In general, there exist two points of peak stress concentration in each T-joint, 180 degrees apart (see Fig. 7). The first crack was found at either one of these points. As the number of cycles increased, the second crack developed at the other point of stress concentration.

Most of the cracks propagated along the toe of the welds. When the first and second cracks extended to a certain length, a portion of the chord wall at the crown was suddenly torn in a fashion similar to a static failure. Typical failure mode for specimens B and F is shown in Figs. 9 and 10. Figure 10 depicts the propagation of fatigue crack. The surface of the crack at the center section of the chord was smoother than the portions where the crack extended. The appearance of chord wall at the crown after the failure of the specimen

was similar to a fracture due to a static tensile force. For the specimens with β ratio of almost 1, the cracks propagated in a somewhat different way. (See Fig. 11).

The propagation of the fatigue cracks was rather slow. The number of cycles to detectable crack initiation was about half of that to complete failure (see Table 2).

The stress distribution patterns in the joints changed after the cracks were initiated at the points of stress concentration. In Fig. 8 the distribution of circumferential stress in the chord surface at the preliminary static load, at the initiation of crack and at some cycles after crack initiation is shown. After a crack was formed, the stresses at the toe of the weld in the circumferential direction seem to vanish. The gradient of stress near the weld toe becomes less as the number of cycles increases after crack formation. The longitudinal strains in the brace near the brace to chord welds were measured and are shown in Fig. 12. During the preliminary static test, negative values of the longitudinal strains near the crown of the chord were noted. After the formation of the first crack the strain at the point near the crack, however, began to decrease and the strains at the other points began to increase. At that instant the highest strain was observed at the second point of stress concentration, and subsequently the second crack was found at that point. After the formation of the second crack, the strains near the crown of the chord became positive. Similar trends were observed in the tests of large-size specimens F (Fig. 13).

The test results indicate that the stress redistribution occurs after the crack formation. The portions of the specimens other than

those near the cracks carry more loads. As the cracks were developed, the stiffness of the joint as a whole decreased. The change in stiffness was not sudden as seen in the load-to-overall deformation curves in Fig. 14.

3.4 Static Failure

The failure pattern of small-size specimens under static loads was quite different from that reported in References (2) and (3). The chords sustained large bending deformations. The chord walls located around the weld lines were finally torn in a manner similar to tension failure (Fig. 15). The large-size specimens tested previously[2, 3] failed by complete separation at the base metal of the chord. The difference is most likely due to the high ductility (62% elongation) of the material of the small-size specimens. The average stresses in the shear area of the small-size specimens at ultimate loads were approximately twice as much as those of the large-size specimens.

4. FATIGUE STRENGTH

4.1 S-N Curves

The stress concentration, as mentioned earlier, is the important factor affecting the fatigue strength of tubular T-joints. The stress concentration factor varies with the geometrical parameters, such as the β and γ ratios, and the cross-sectional shape of the brace-to-chord weld. To investigate the effects of the β and γ ratios on the fatigue strength of the T-joints, S-N curves were established for each type of the specimens.

The relationships of average stress "S" in the shear area to the number of cycles "N" for crack initiation or complete failure are presented on semi-logarithmic coordinates in Figs. 16 through 24. The solid lines drawn in these figures are the S-N curves fitted by the method of least squares, in which the quantity S was assumed to have homogeneous variance for the reversal test results of B specimens (Figs. 17 and 18), while, for the rest of the S-N curves, the quantity log N was assumed to have homogeneous variance. The technique used for this curve fitting is the same as that described in Reference (4).

It is seen from these figures that the test results are scattered considerably. In most of the S-N diagrams, however, there seems to exist certain correlation between S and N, which is typical of S-N relationships in the fatigue of metal structures.

It is possible to estimate the fatigue strength for each type of specimen from the fitted S-N curves. The fatigue strength at 10^5 and 2×10^5 cycles obtained by this method is shown in Table 4. Most of

the S-N curves cover the above range of cycles. Only a few scattered data points for specimens D were available and those points are shown in Fig. 23. For specimens E the S-N curve (Fig. 24) was extended to cover the range of cycles mentioned earlier.

4.2 Effects of β and γ Ratios

The stress concentration factor of T-joints varies with β and γ ratios. According to an empirical formula, Eq. 66 in Reference 3, based on the test results of References (2) and (3), the values of stress concentration factor for the specimens discussed here are as shown in Table 5. The stress concentration factor obtained from theoretical analysis is also shown in Table 5. The distribution of circumferential stresses, based on the theoretical analysis, at the center section of the chord, when the brace is subjected to an axial force of 1 kip, is shown in Fig. 25.

The variation of stress concentration factor with respect to β has a common trend in both the experimental and theoretical values (Table 5). However, these magnitudes for the stress concentration factors differ considerably from each other. The stress concentration factor is greatest for specimen Type C ($\beta = 0.656$), and decreases as β increases.

The relationships between β and the fatigue strength are given in Table 4 and are illustrated in Fig. 26. The fatigue strength is lowest for specimen B ($\beta = 0.432$). Specimens A ($\beta = 0.216$) and C ($\beta = 0.656$) have higher fatigue strength. The fatigue strength of specimens D ($\beta = 0.885$) was not obtained. It seems logical from Fig. 23 to infer that the fatigue strength of specimens D is higher than that of specimens C. In

summary the fatigue strength takes the lowest value around $\beta = 0.43$, and increases as β increases.

The fatigue strength to β relationships generally agree with the relationships between the stress concentration factor and β, since the fatigue strength should decrease as the stress concentration factor increases. However, it should be noted that the stress concentration factors in Table 5 are not fully reliable. The computed stresses for specimen A, for instance, contain considerable errors because the number of terms of the series used in the numerical calculation was not large enough (see Table 5 and Fig. 25). The experimental equation[2], [3] was based on test results which covered limited ranges of α, β, γ and τ ratios, and which required an extrapolation to obtain stresses in the specimens tested at the toe of the weld.

The fatigue strength became higher as γ ratio was decreased. This is seen in Table 4 by comparing specimens B ($\gamma = 24$) and E ($\gamma = 14$). The stress concentration factor is smaller for specimen E than for specimen B. This agrees with the fatigue behavior.

The modified Goodman diagram in Fig. 27, illustrates the fatigue strength of specimens B for lives of 10^5 and 2×10^5 cycles. The static strength shown in the figure is that of specimen 4 in Ref. (2) instead of the static strength of B specimens. The fatigue failure mode of B specimens was closer to the failure mode of specimen 4 under static loading. The ratios α, β and γ are almost identical for specimen 4 and specimens B.

The fatigue strength of specimens F was considerably smaller than that of specimens B, in spite of the fact that both types had almost equal α, β, γ and τ ratios and, therefore, almost equal stress concentration factors. The fatigue resistances of specimens B and F are

compared in Fig. 28 along with the load deformation curve of specimen 4 under static load. The S-N relationships of specimens F are shown in Fig. 20 along with specimens B. The test results indicate that the fatigue strength of specimens F is approximately 60% of the fatigue strength of specimens B.

The size-effect as revealed here can be attributed to many factors. In general the fatigue strength of a larger member may be expected to be lower than that of a smaller member because the larger member has statistically the greater opportunity to contain flaws. Furthermore, the cross sectional shapes of the weld are different between specimens B and F (Figs. 29a, b). The convex face of welds in specimens F may have caused a greater stress concentration at the toe of the weld than the concave one as in specimens B. In addition, the strains at the critical points could have been beyond the elastic limit. These and other various factors might have had considerable impact on the size-effect observed in this investigation.

5. SUMMARY AND CONCLUSIONS

5.1 Summary

In this report the results of fatigue tests of tubular T-joints were discussed. The specimens consisted of two series:

1. About one hundred small-size specimens of various β and γ ratios subjected to certain patterns of stress cycles (R =-1.0, 0.0, 0.16 and 0.5).
2. Three large-size specimens to compare with the fatigue behavior of small-size specimens. For these specimens R=0.16.

5.2 Conclusions

1. The stress concentration was considered as the important factor influencing the fatigue behavior. The points of highest stress concentration in the chord walls are at the toe of the welds. The fatigue cracks initiated at these points and crack propagation was rather slow along the weld toe possibly because of stress redistribution. The joints survived approximately twice the number of cycles to crack initiation.
2. The fatigue strength expressed in terms of the average stress in the shear area was obtained from the S-N curves of the small-size specimens. The fatigue strength to β relationships were shown in a concave-upward curve having the lowest fatigue strength around β = 0.43. The variation of the fatigue strength due to β was not very

critical from the view point of an actual design. The fatigue strength increased as ratio was decreased.

3. From the results of three large and about a hundred small size specimens tested it appears that there is a size effect which is not negligible and should be considered.

4. The tests should be extended to a more comprehensive investigation using large-size specimens. The fatigue strength at the lower range of cycles was considered since the number of cycles of peak loads which would be applied to the offshore structures may be rather limited.

REFERENCES

(1) The Use of Structural Steel in Building, B.S., 449: 1959, British Standard Institution, p. 93.

(2) J. S. Noel, L. A. Beale and A. A. Toprac, "An Investigation of Stresses in Welded T-Joints," Report No. S. F. R. L. Tech. Rpt. P550-3, The University of Texas (March 1965).

(3) L. A. Beale and A. A. Toprac, "Research in Tubular Connections: Analysis of T, Y, and K Welded Tubular Connections," Report No. S. F. R. L. Tech. Rpt. P 550-9, The University of Texas (April 1967).

(4) W. Weibull, "Fatigue Testing and Analysis of Results," Pergamon Press (1961), Section 91.

Table 1 Specimen Details

Specimen Type	Chord O. D. D (in.)	Chord Thickness T (in.)	Brace O. D. d (in.)	Brace Thickness t (in.)	Chord Length L (in.)	(L/a) α	(C/a) β	(a/T) γ	(t/T) τ	Size of Welds Sc (in.)	Size of Welds SL (in.)	Shear Area (in.^{2})
A	2.25	0.046	0.51	0.035	9.0	8.17	0.216	24.0	0.761	0.134	0.137	**0.0737**
B	"	"	1.00	0.047	"	"	0.432	"	1.00	0.094	0.116	**0.146**
C	"	"	1.50	0.055	"	"	0.656	"	1.20	0.092	0.147	**0.226**
D	"	"	2.00	0.050	"	"	0.885	"	1.09	0.056	0.148	**0.319**
E	"	0.077	1.00	0.047	"	7.36	0.439	14.1	0.597	0.103	0.130	**0.245**
F	8.61	0.189	3.77	0.192	35.0	8.31	0.425	22.3	1.02	0.243	0.291	**2.26**

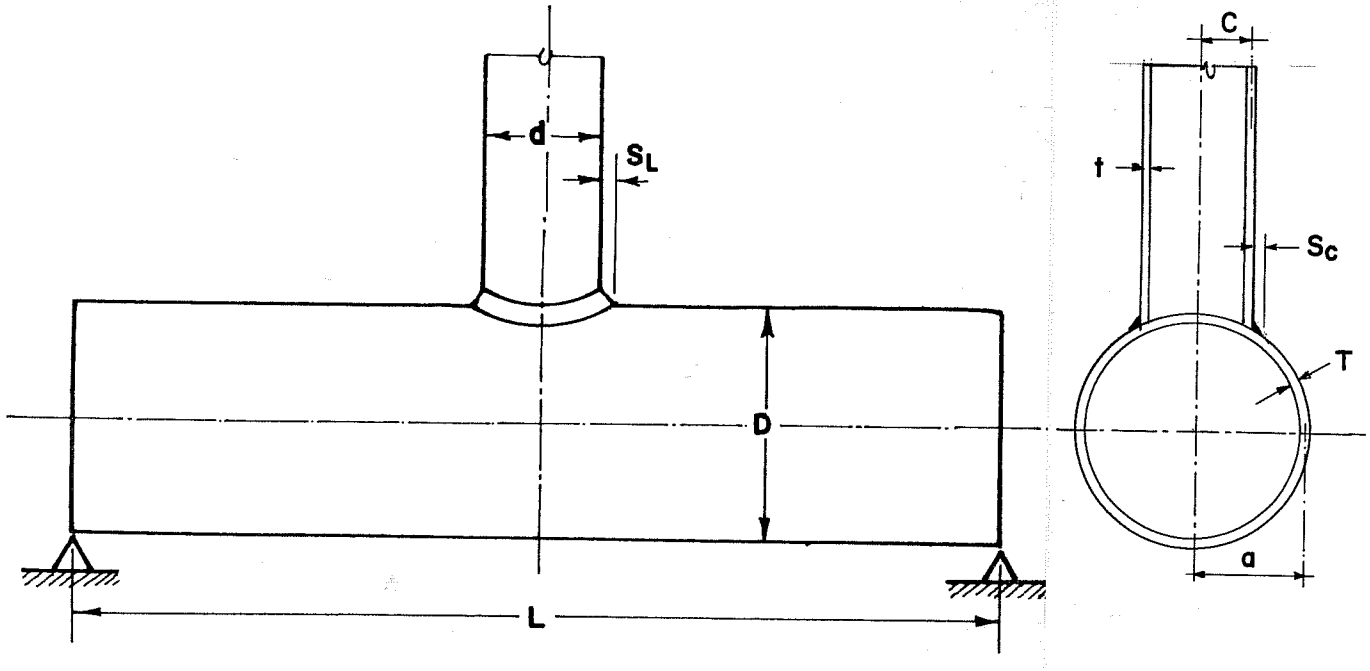

TABLE 2. SUMMARY OF TEST RESULTS

SPEC. NO.	AMPLITUDE OF LOAD (lbs)	$R = \frac{S_{min}}{S_{max}}$	STRESS AMPLITUDE (KSI)	NUMBER OF CYCLES TO INITIAL CRACK	NUMBER OF CYCLES TO 2ND CRACK	NUMBER OF CYCLES TO FAILURE	REMARKS
A-1	278	-1.0	3.77	244,800	—	276,500	
A-2	245	〃	3.33	82,200	> 288,000	337,700	
A-3	278	〃	3.77	247,500	> 288,000	337,700	
A-4	311	〃	4.23	27,900	> 36,000	39,300	
A-5	〃	〃	〃	35,700	> 50,900	57,000	
A-6	〃	〃	〃	48,300	> 81,000	100,900	
A-7	278	〃	3.77	50,400	> 98,000	123,800	
A-8	245	〃	3.33	1,881,000	> 2,096,600	2,125,000	
A-9	〃	〃	〃	239,600	> 284,400	395,300	
A-10	311	〃	4.23	45,300	> 82,800	89,900	
B-1	570	-1.0	3.90	16,800	40,400	43,300	
B-2	430	〃	2.94	—	—	1,276,000	
B-3	360	〃	2.46	182,000	—	682,800	
B-4	430	〃	2.94	—	—	1,775,500	CRACK PROPAGATED TO THE BRACE ALONG THE UNDER-CUT OF THE WELD
B-5	〃	〃	〃	111,100	> 260,000	335,900	
B-6	〃	〃	〃	66,000	160,000	162,200	
B-7	〃	〃	〃	120,000	—	162,000	
B-8	291	〃	1.99	—	—	> 7,677	RUN-OUT SPECIMEN
B-9	360	〃	2.46	—	—	344,600	
B-10	570	〃	3.90	32,160	39,100	41,600	
B-11	430	〃	2.94	127,900	203,300	229,100	
B-12	570	〃	3.90	18,100	—	50,900	
B-13	430	〃	2.94	206,800	>287,900	372,200	
B-14	901	〃	6.16	1,100	2,100	2,200	
B-15	703	〃	4.81	7,700	—	19,800	
B-16	901	〃	6.16	2,300	4,900	5,800	
B-17	703	〃	4.81	5,600	7,300	10,100	First Crack was off-center.

TABLE 2 (CONT'D)

SPEC. NO.	AMPLITUDE OF LOAD (lbs)	$R = \frac{S_{min}}{S_{max}}$	STRESS AMPLITUDE (ksi)	NUMBER OF CYCLES TO INITIAL CRACK	NUMBER OF CYCLES TO SECOND CRACK	NUMBER OF CYCLES TO FAILURE	REMARKS
B-18	570	-1.0	3.90	34,900	54,700	60,100	
B-19	901	〃	6.16	3,000	3,400	6,000	
B-20	570	〃	3.90	29,500	31,200	45,400	
B-21	703	〃	4.81	3,300	7,100	8,600	
B-22	421	-0.0082	2.88	70,300	>80,000	98,200	
B-23	407	-0.0087	2.78	95,400	> 112,500	134,800	
B-24	421	-0.0157	2.92	34,800	> 52,300	74,200	
B-25	407	-0.0087	2.78	53,100	53,400	82,500	
B-26	394	-0.0093	2.70	71,500	> 138,200	198,700	
B-27	407	-0.0082	2.78	75,600	114,600	131,900	
B-33	342	0.4940	2.34	193,500	> 277,500	334,700	
B-34	396	0.4931	2.71	76,900	> 108,000	143,500	
B-35	〃	〃	〃	168,700	182,200	212,600	
B-36	339	0.1547	2.32	104,100	165,600	184,200	
B-37	〃	〃	〃	138,000	>206,800	282,600	FIRST CRACK $\frac{3''}{16}$ OFF CENTER
B-38	407	0.1581	2.78	89,400	107,000	127,600	
B-39	〃	〃	〃	81,000	81,100	108,000	
B-40	475	0.1613	3.25	37,000	53,200	59,300	
B-41	〃	〃	〃	27,800	37,700	49,700	
B-42	〃	〃	〃	28,500	31,900	42,900	
B-43	353	-0.0110	2.41	83,100	> 176,800	231,300	
B-44	451	0.4939	3.08	177,800	> 208,300	247,300	
B-45	〃	〃	〃	157,900	> 176,400	229,400	
B-46	353	-0.0110	2.41	243,200	> 297,200	369,600	
B-47	407	0.1581	2.78	45,900	> 97,300	107,900	
B-48	339	0.1547	2.32	163,800	255,800	291,500	
B-49	360	-1.0	2.46	93,300	> 154,000	312,800	FIRST CRACK $\frac{3''}{16}$ OFF CENTER
B-50	703	〃	4.81	12,400	20,000	23,500	

TABLE 2 (CONT'D)

SPEC. NO.	AMPLITUDE OF LOAD (lbs)	$R = \frac{S_{min}}{S_{max}}$	STRESS AMPLITUDE (ksi)	NUMBER OF CYCLES TO INITIAL CRACK	NUMBER OF CYCLES TO SECOND CRACK	NUMBER OF CYCLES TO FAILURE	REMARKS
B-51	543	0.1624	3.71	21,800	> 25,100	34,100	
B-52	"	"	"	21,900	> 34,200	39,100	
B-53	360	−1.0	2.46	184,200	> 266,400	412,800	
B-54	—	—	41.56	—	—	—	STATIC TEST
B-55	—	—	37.18	—	—	—	STATIC TEST
BP-2	291	−1.0	1.99	—	—	7,180,900	
BP-3	703	"	4.81	5,000	—	13,600	
BP-4	901	"	6.16	3,500	—	3,600	
C-1	743	−1.0	3.29	72,000	247,700	481,900	
C-2	850	"	3.76	25,500	65,300	68,600	
C-3	"	"	"	24,000	34,900	36,200	
C-4	"	"	"	23,500	66,000	66,400	
C-5	743	"	3.29	44,300	81,100	103,600	
C-6	"	"	"	49,000	66,000	101,100	
C-7	639	"	2.83	121,200	158,600	240,600	
C-8	"	"	"	88,500	> 220,000	242,600	
C-9	743	"	3.29	32,200	> 108,000	137,000	
C-10	639	"	2.83	263,000	503,700	883,600	
D-1	960	−1.0	3.00	387,000	> 648,000	657,800	
D-2	848	"	2.66	216,000	> 464,000	531,500	
D-3	711	"	2.23	3,501,000	—	4,104,000	
D-4	960	"	3.00	1,672,200	1,951,200	1,963,620	FIRST CRACK $\frac{1}{2}$" OFF CENTER
D-7	"	"	"	2,824,200	—	4,324,350	
E-1	896	−1.0	3.66	58,600	> 79,500	137,200	
E-2	960	"	3.92	234,000	> 266,400	293,000	

TABLE 2 (CONT'D)

SPEC. No.	AMPLITUDE OF LOAD (lbs)	$R = \frac{S_{min}}{S_{max}}$	STRESS AMPLITUDE (KSI)	NUMBER OF CYCLES TO INITIAL CRACK	NUMBER OF CYCLES TO SECOND CRACK	NUMBER OF CYCLES TO FAILURE	REMARKS
E-3	960	-1.0	3.92	477,000	498,600	502,400	
E-4	896	"	3.66	477,000	>504,000	568,800	
E-5	"	"	"	765,000	—	799,800	
E-6	784	"	3.20	1,517,400	—	1,809,300	
E-7	"	"	"	3,152,000	—	>3,210,900	FAILURE AT CONNECTING FIXTURE
E-8	960	"	3.92	230,400	—	257,800	
E-9	896	"	3.66	>1,060,900	—	>1,060,900	FAILURE AT CONNECTING FIXTURE
E-10	"	"	"	333,000	> 419,400	480,600	
E-11	784	"	3.20	—	—	>1,062,000	
E-12	960	"	3.92	378,000	> 423,000	433,800	
E-13	896	"	3.66	169,200	> 216,000	239,600	
E-14	784	"	3.20	142,200	> 194,400	271,800	
E-15	"	"	"	1,161,000	> 1,260,000	1,414,700	
F-1		0.16	2.72	9,060	9,060	11,600	
F-2		"	1.78	40,800	65,870	67,420	
F-3		"	"	57,380	—	78,803	

Table 3 Mechanical Properties of Tubes

Nominal Size (in. or B.W.G.)	O.D. (in.)	Thickness (in.)	Yield Point (ksi)	Tensile Strength (ksi)	Elongation (%)	Material Designation
1/2 X 20	0.51	0.035	54.1	55.9	31	1
1 X 18	1.00	0.048	50.0	53.8	44	2
1 X 18	1.00	0.046	57.8	59.0	31	8
1 1/2 X 17	1.50	0.055		60.8	31	9
2 X 17	2.00	0.050	45.0	51.2	50	10
2 1/4 X 18	2.26	0.047	41.5	50.1	45	3
"	2.25	0.045	37.4	46.8	59	5
"	2.25	0.047	41.0	47.7	50	6
"	2.25	0.046	48.8	53.9	62	7
2 1/4 X 14	2.25	0.077	46.7	54.5	44	4
8 5/8 X 3/16	8.61	0.189	63.5	71.5	19	
3 3/4 X 3/16	3.77	0.192	63.0	79.6	17	

Note: Mechanical properties were determined by standard tension tests according to ASTM A 370. For the tubes in which O.D's are less than 2 1/4", tension test specimens of full size tubular sections were used. For the tubes of 8 5/8" and 3 3/4" O.D., longitudinal tension specimens were cut from the tubes.

Table 4 FATIGUE STRENGTH AT CERTAIN NUMBER OF CYCLES

Specimen Type	Type of Cyclic Loads	Fatigue Strenth "S" (ksi) for Initial Crack 10^5	Initial Crack 2×10^5	Complete Failure 10^5	Complete Failure 2×10^5	β	γ	β' *
A	R= -1	3.84	3.54	4.08	3.76	0.216	24.0	0.276
B	R= -1	2.98	2.62	3.41	3.09	0.432	"	0.475
	R= 0	2.59	2.24	2.87	2.57	"	"	"
	R=0.16	2.50	1.97	2.90	2.41	"	"	"
	R=1/2	—	—	—	3.10	"	"	"
C	R= -1	2.98	2.61	3.50	3.16	0.656	"	0.697
D	R= -1	—	—	—	—	0.885	"	0.910
E	R= -1	4.34	4.03	4.48	4.16	0.439	14.1	0.486

* $\beta' = (d + Sc - t) / (D - T)$

Table 5 Stress Concentration Factor

Specimen Type	β	Stress Concentration Factor	
		Test*	Theoretical Analysis
A	0.216	19.8	4.30
B	0.432	24.5	15.3
C	0.656	27.2	17.9
D	0.885	17.6	10.5
E	0.439	11.8	----
F		26.8	14.2

* According to Eq. 66 in Reference (3).

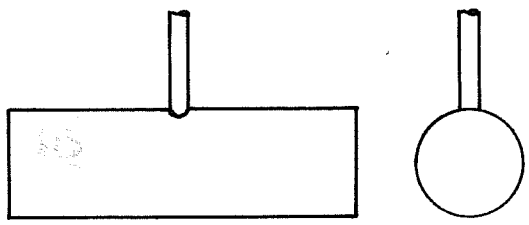

TYPE A (β = 0·38)

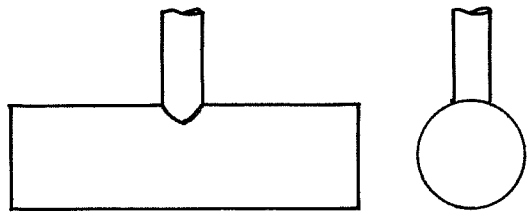

TYPE B,E,F (β ≒ 0·43)

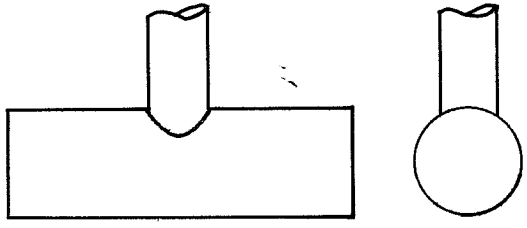

TYPE C (β = 0·66)

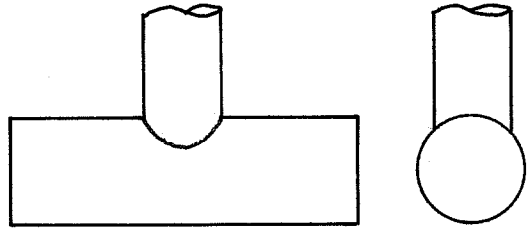

TYPE D (β = 0·88)

FIG. 1 SPECIMEN CONFIGURATION.

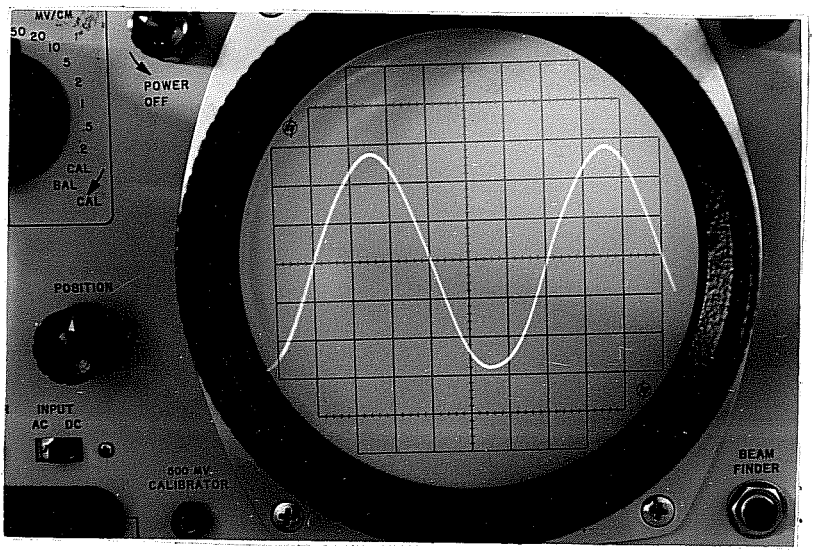

Fig. 2 Dynamic Load Applied by Sonntag Fatigue Machine (Reversal Test)

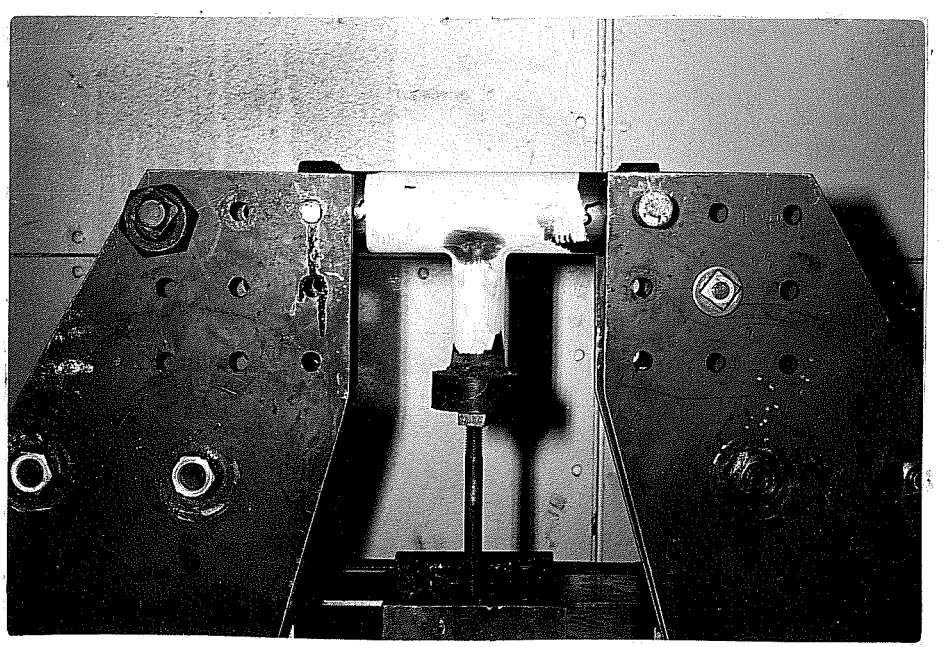

Fig. 3 Test Set-up for Small-size Specimens (Black spot is the kerosene spread from the crack.)

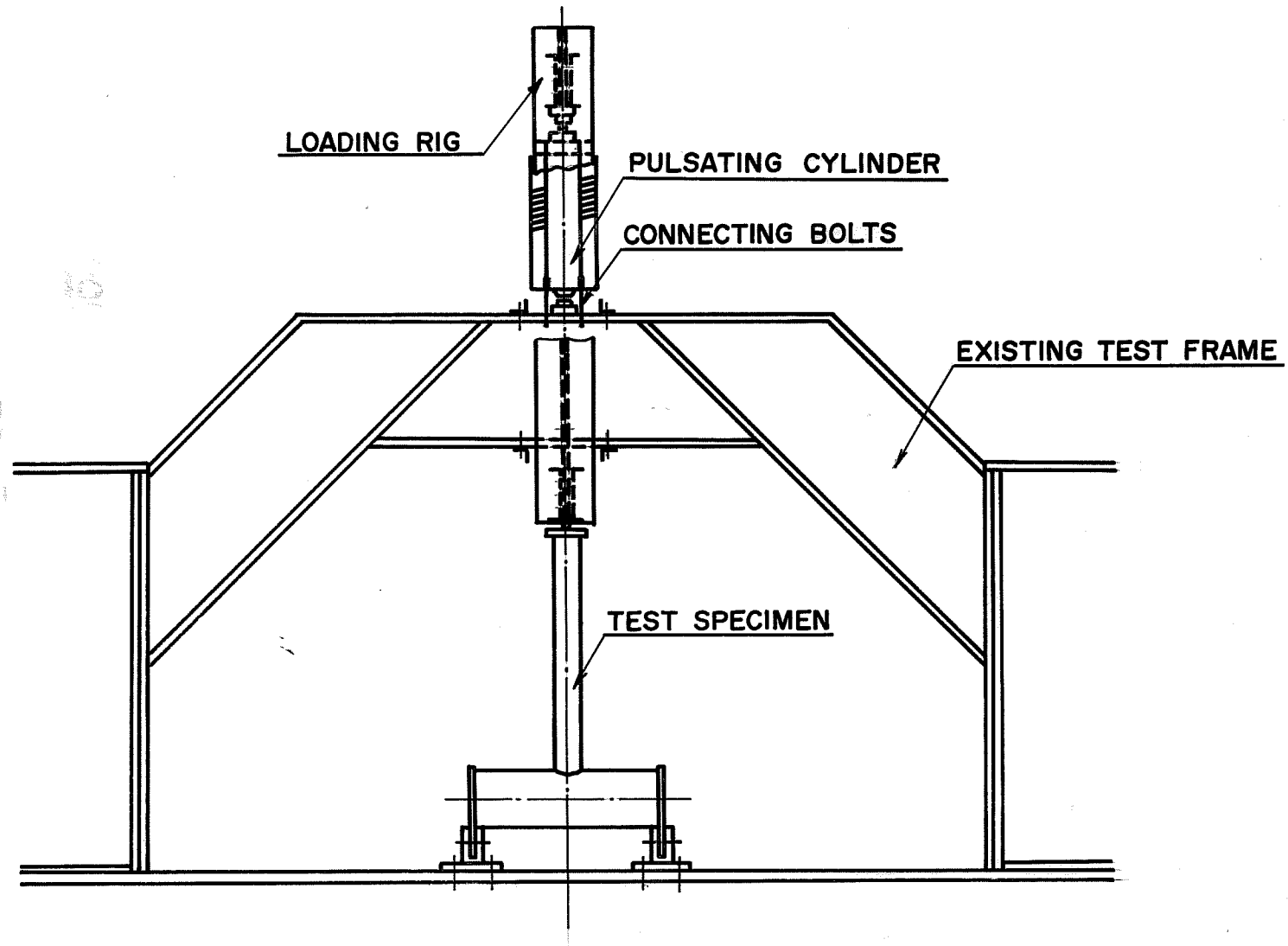

FIG. 5 TEST SET-UP FOR LARGE-SIZE SPECIMENS

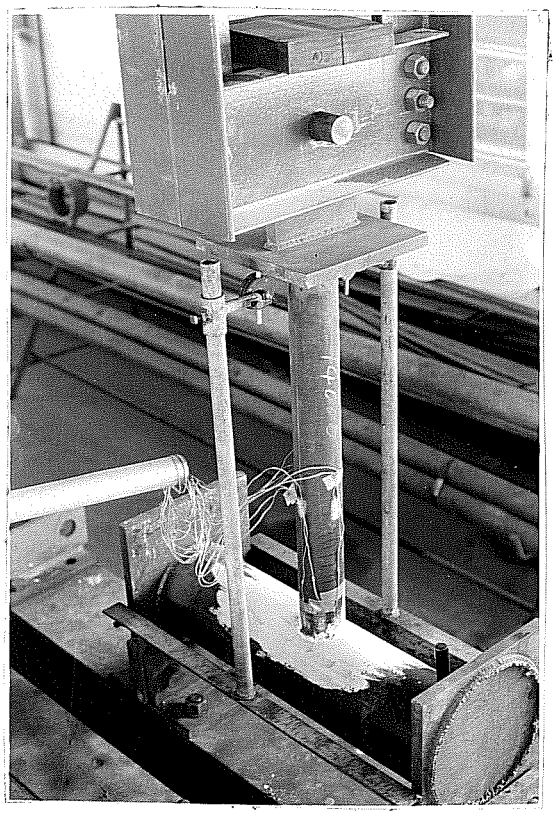

Fig. 6 Test Set-up for Large-size Specimens

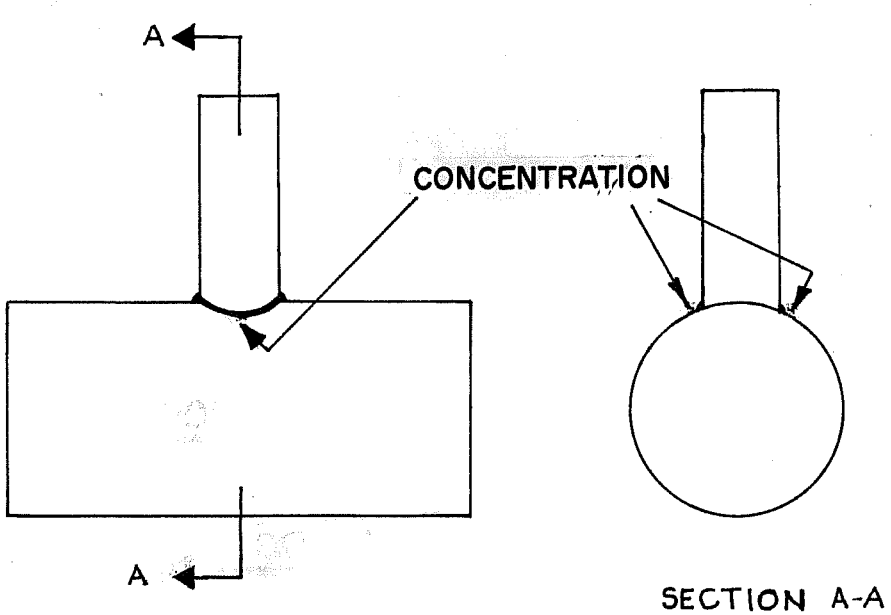

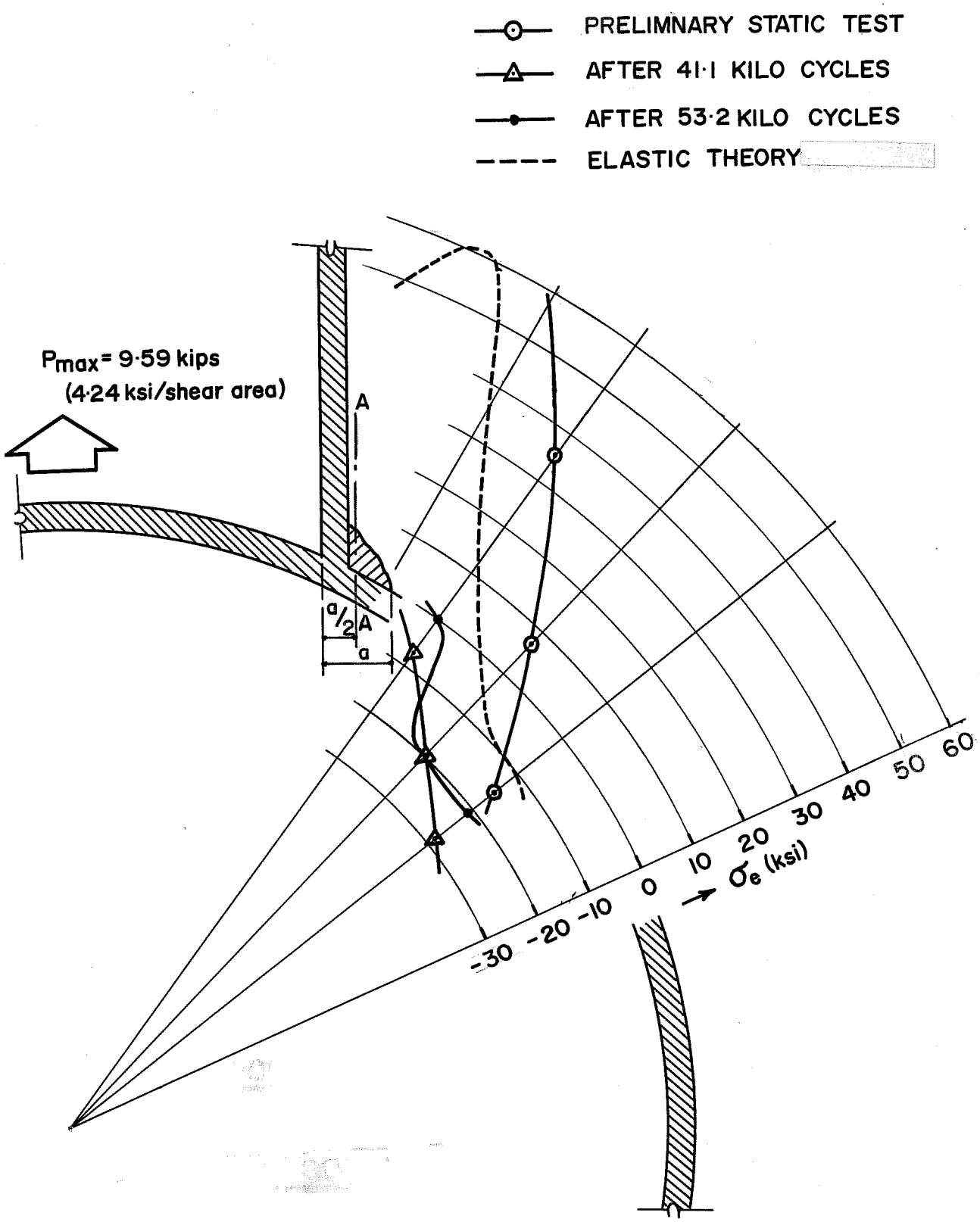

FIG. 8 CIRCUMFERENTIAL STRESS DISTRIBUTION ON THE CHORD SURFACE (SPECIMEN F-2)

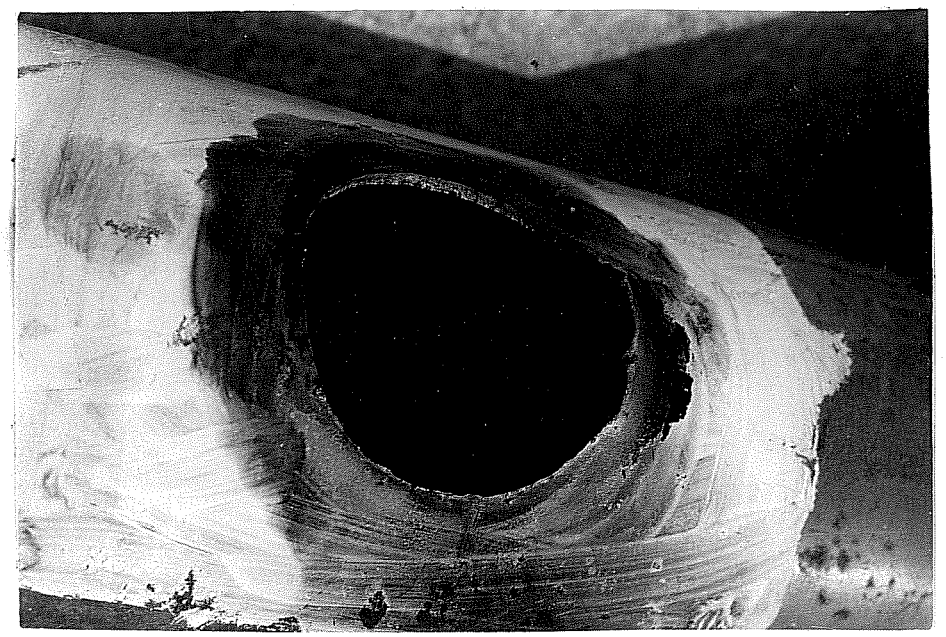

Fig. 10 Specimen Type F after Failure

Fig. 11 Specimen Type D after Failure

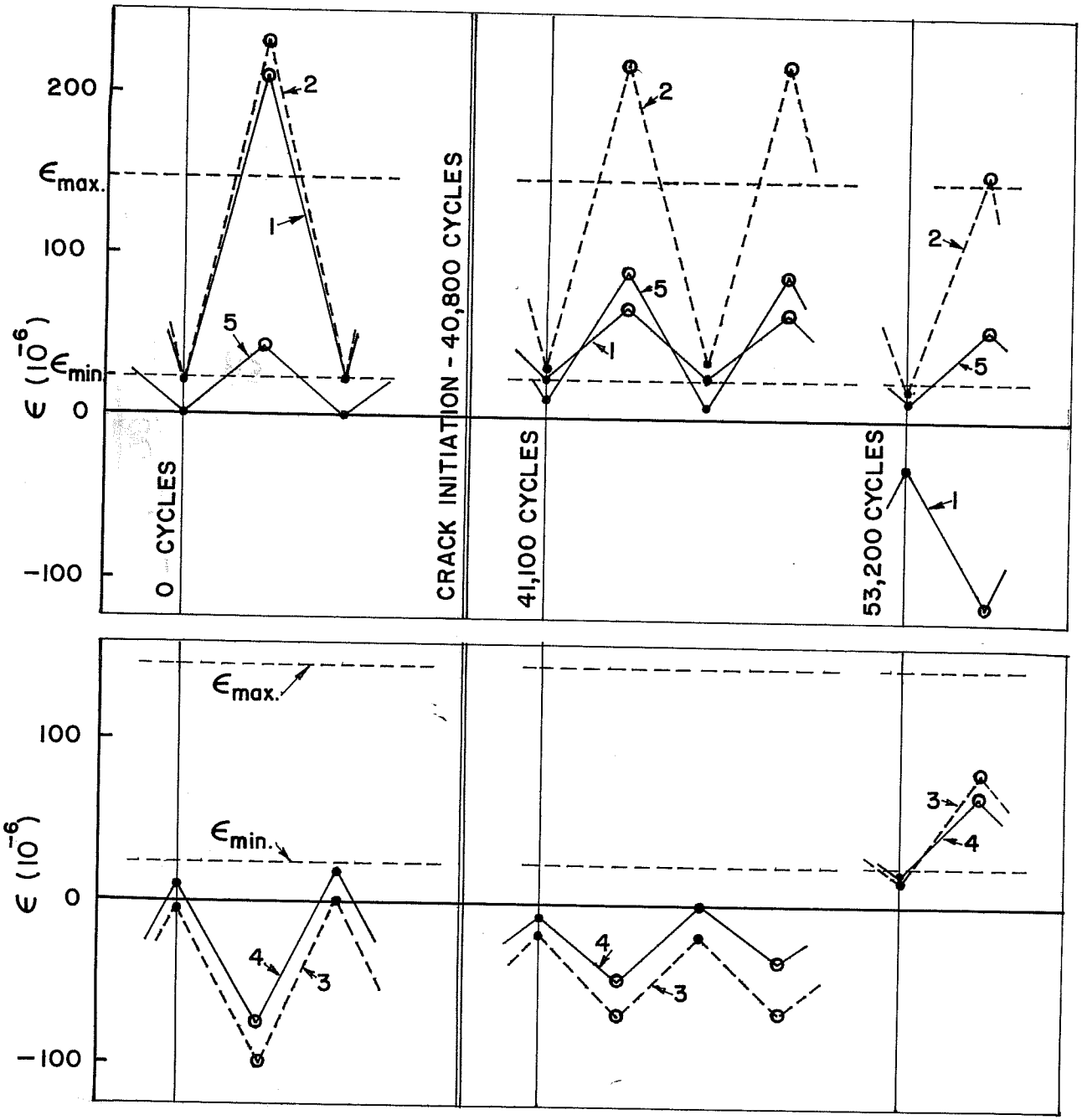

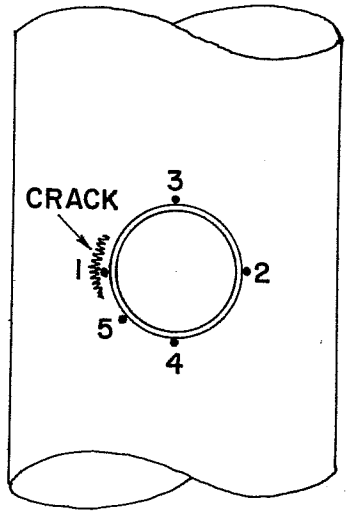

STRAIN GAGE LOCATIONS

⊙ STRAIN AT MAXIMUM LOAD

● STRAIN AT MINIMUM LOAD

FIG. 13 STRAIN Vs CYCLE DIAGRAM (SPECIMEN F-2)

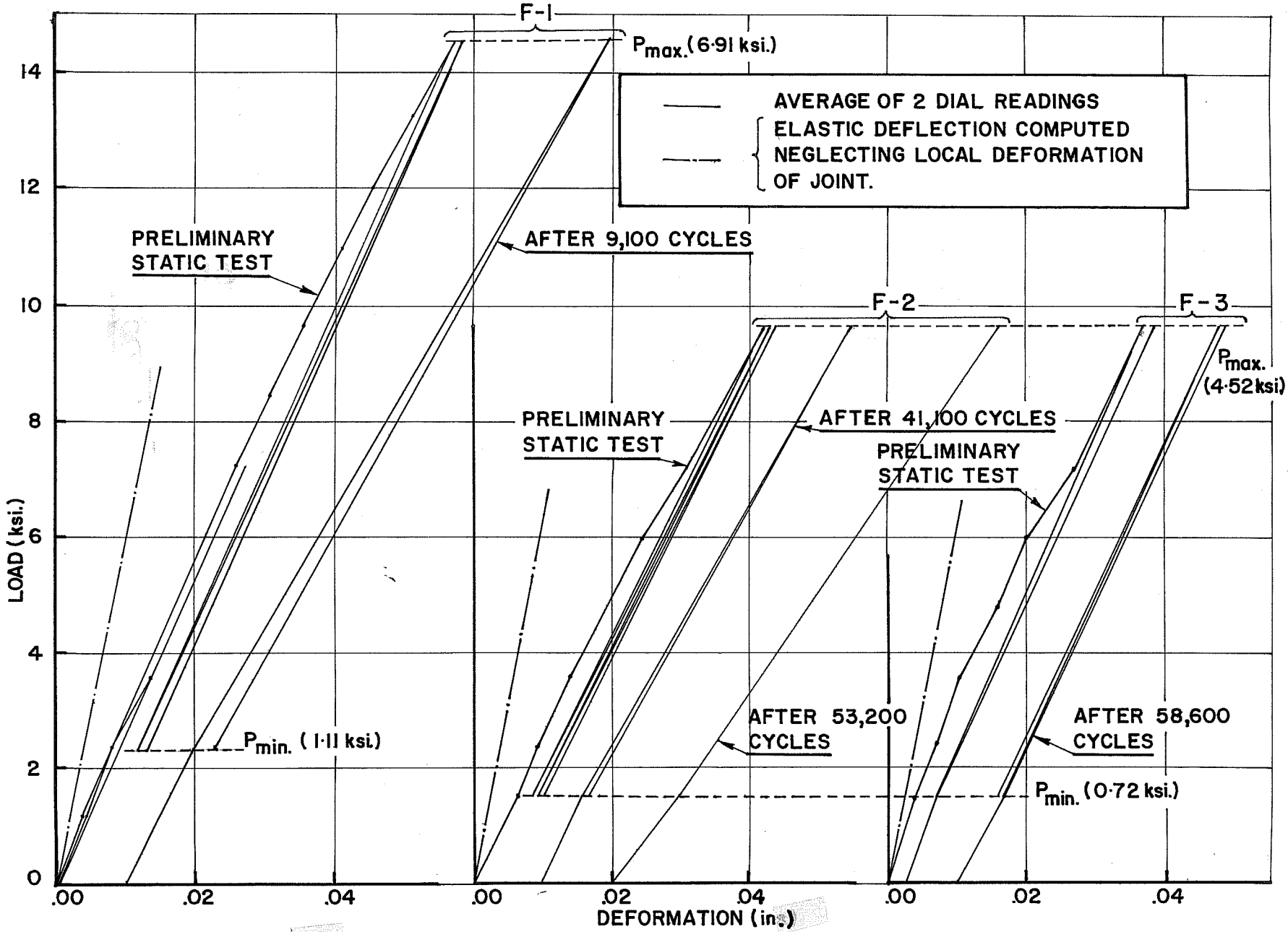

FIG. 14 OVERALL DEFORMATION OF TYPE F SPECIMENS

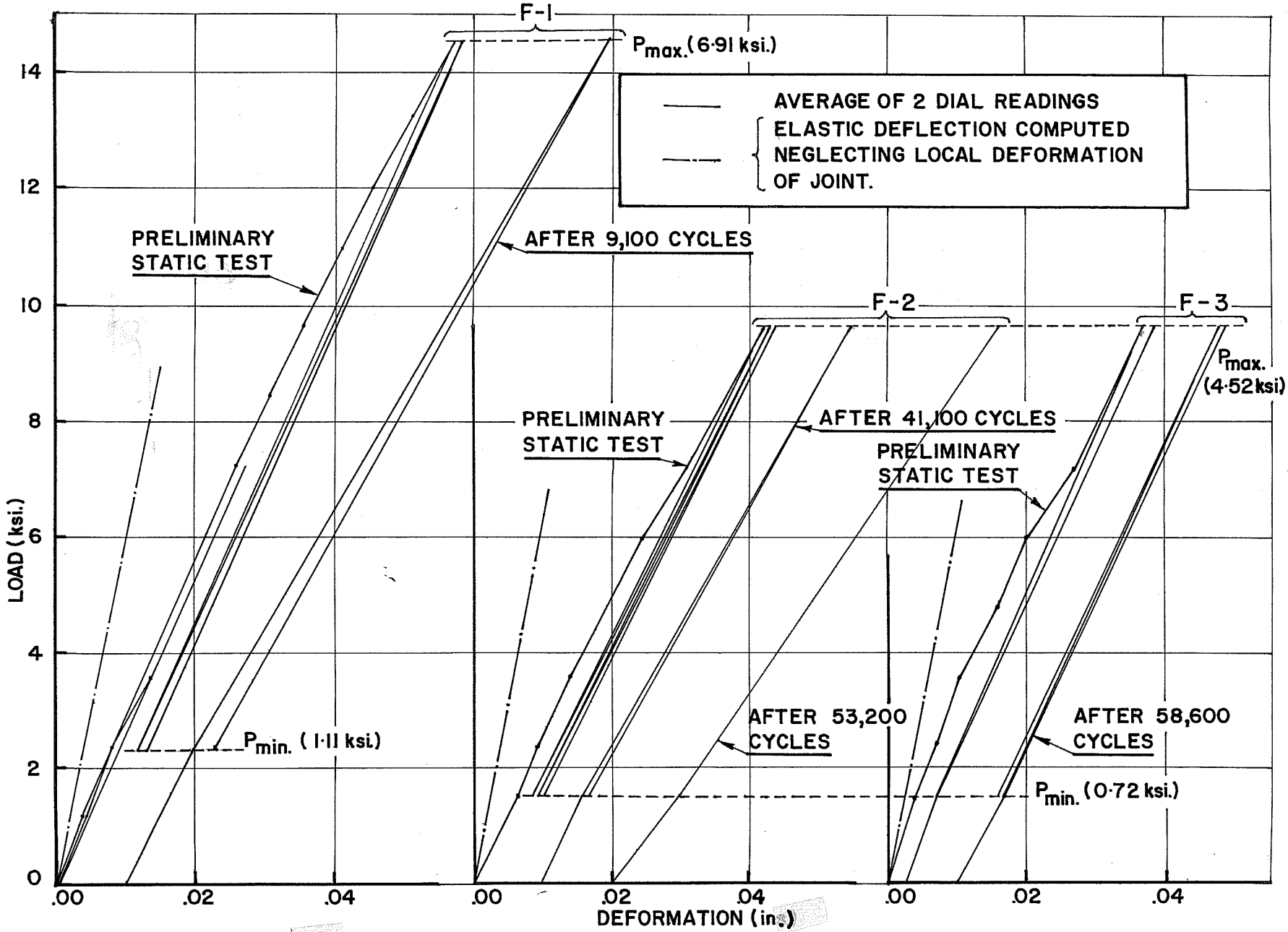

FIG. 14 OVERALL DEFORMATION OF TYPE F SPECIMENS

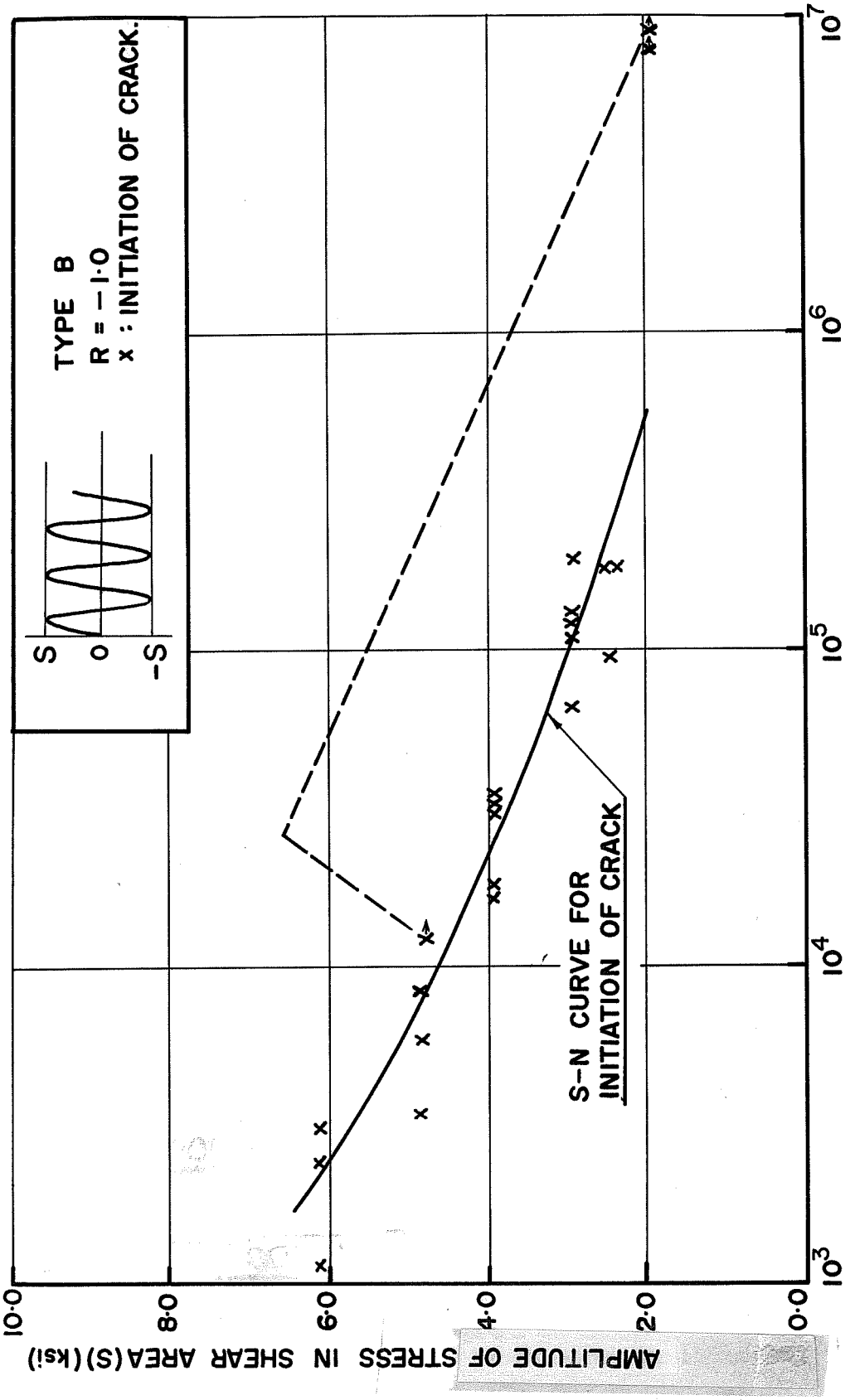

FIG. 17 S–N DIAGRAM FOR TYPE B SPECIMENS

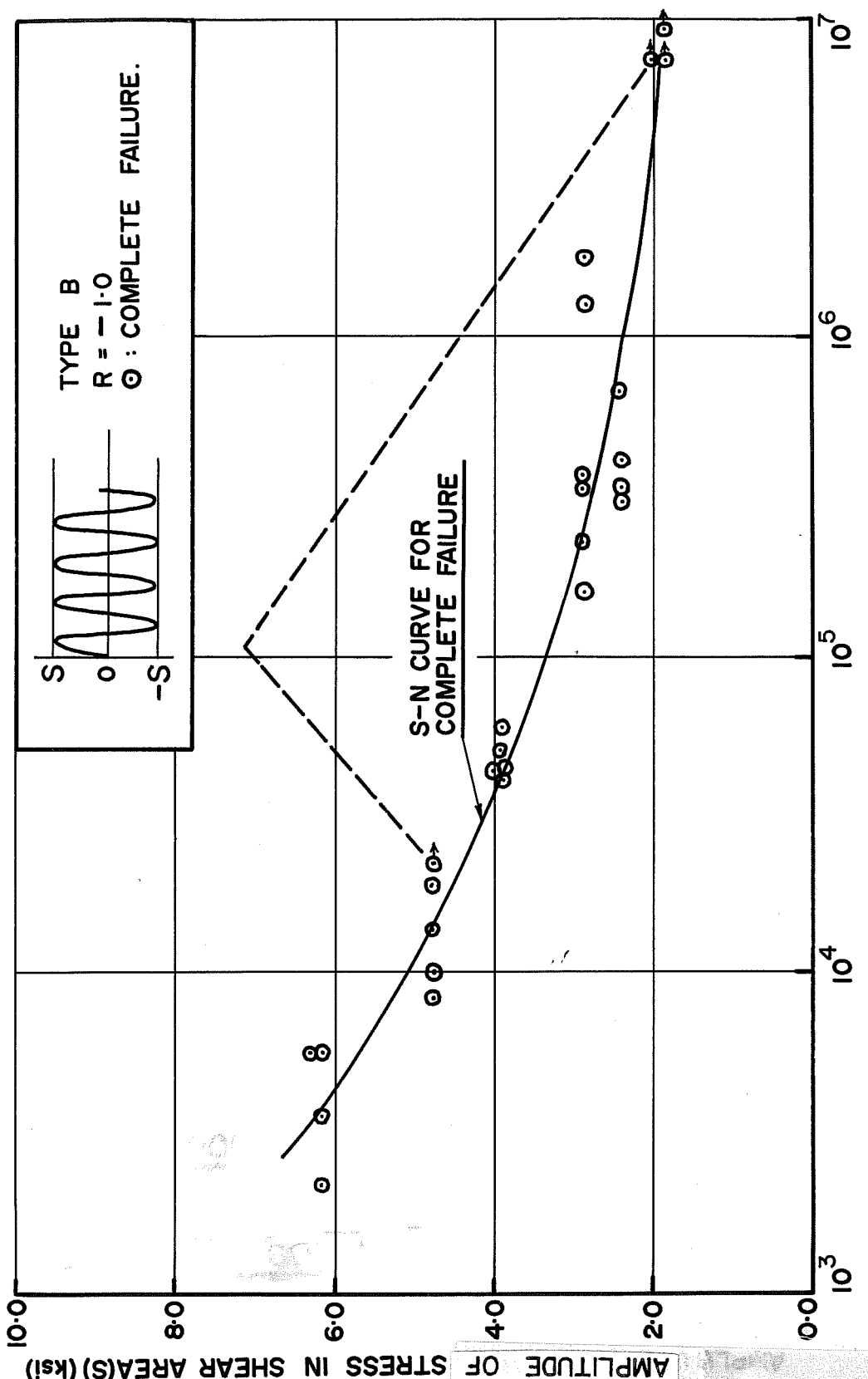

FIG. 18 S–N DIAGRAM FOR TYPE B SPECIMENS

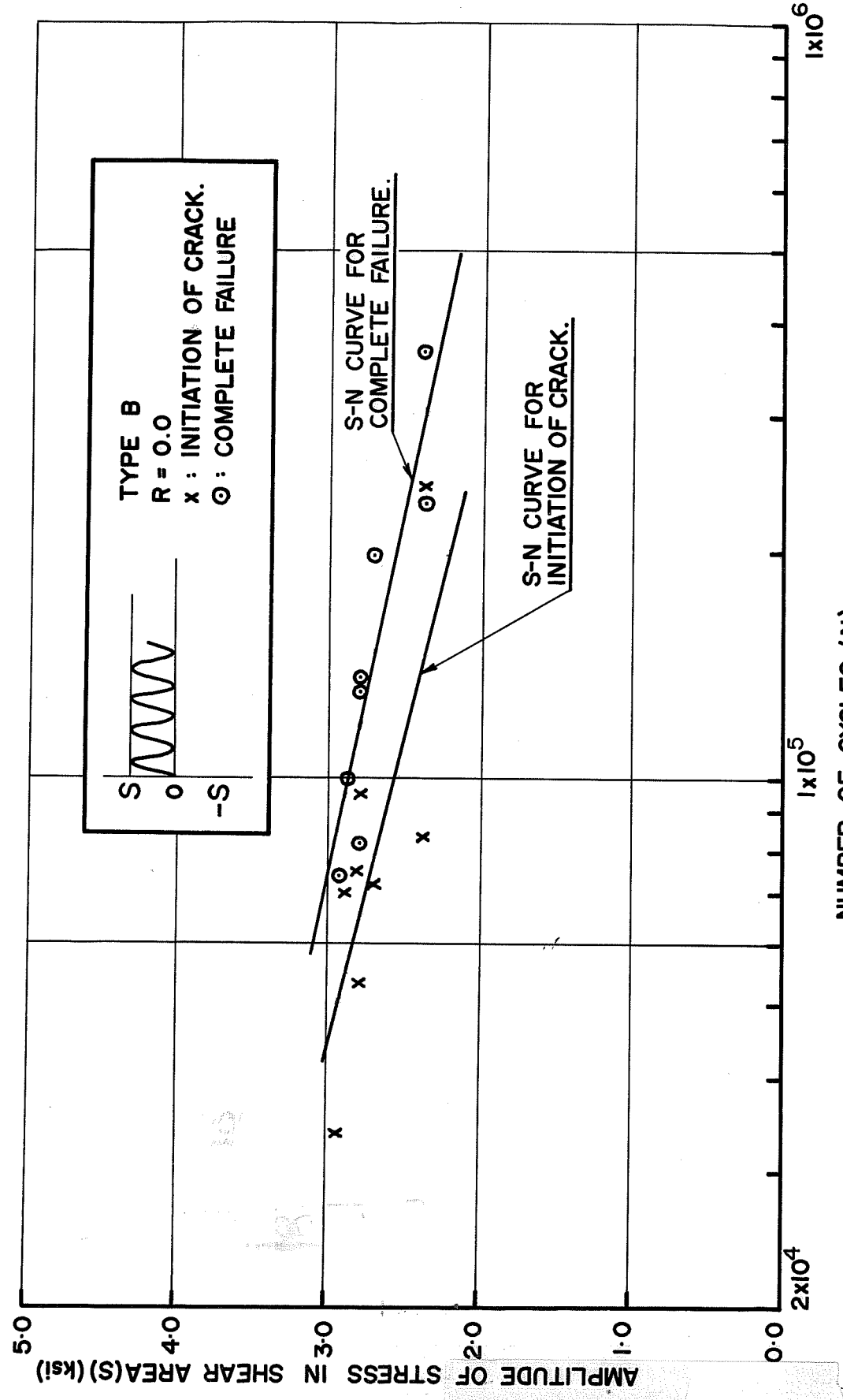

FIG. 19 S-N DIAGRAM FOR TYPE B SPECIMENS

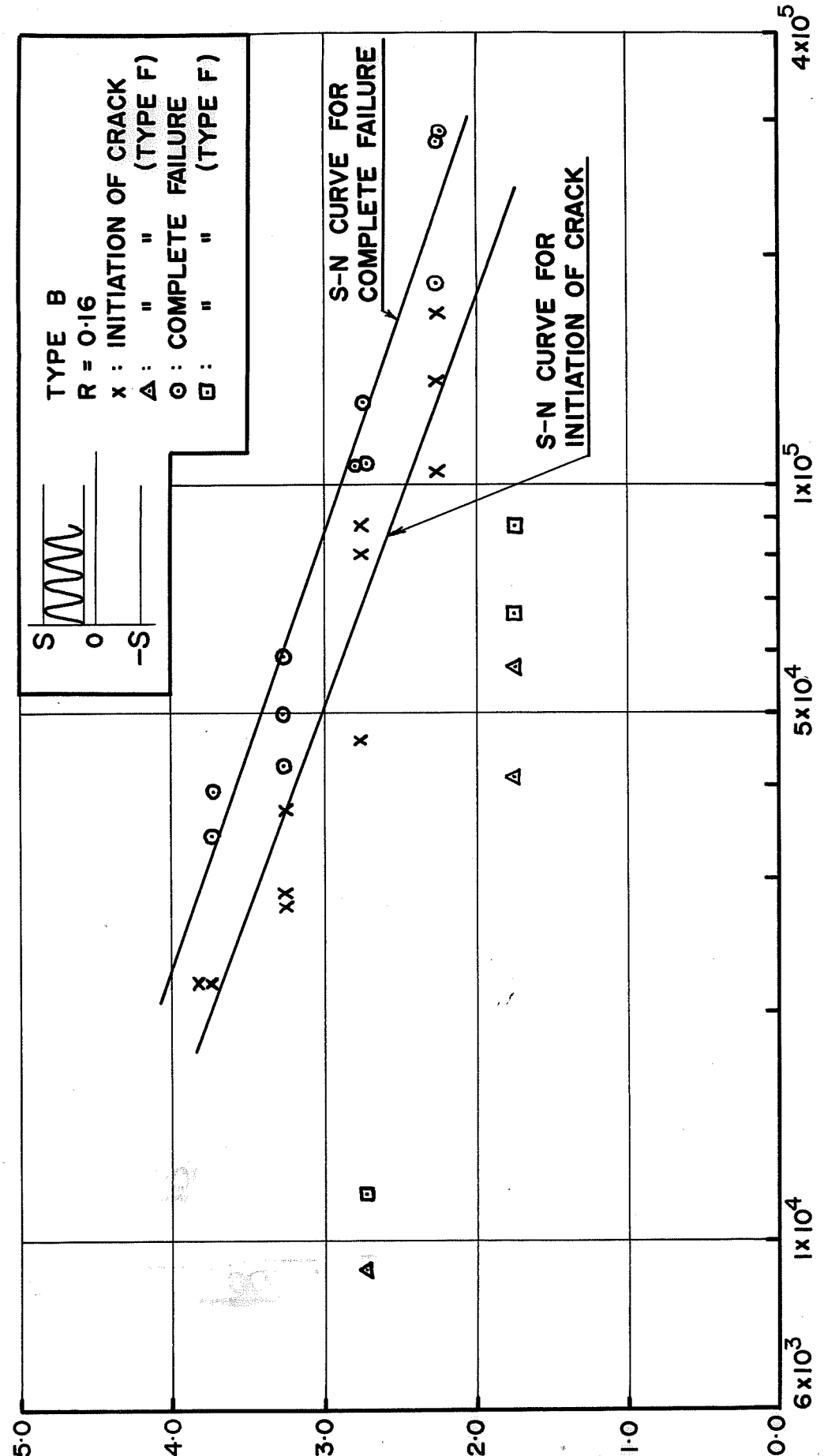

FIG. 20 S–N DIAGRAM FOR TYPE B SPECIMENS

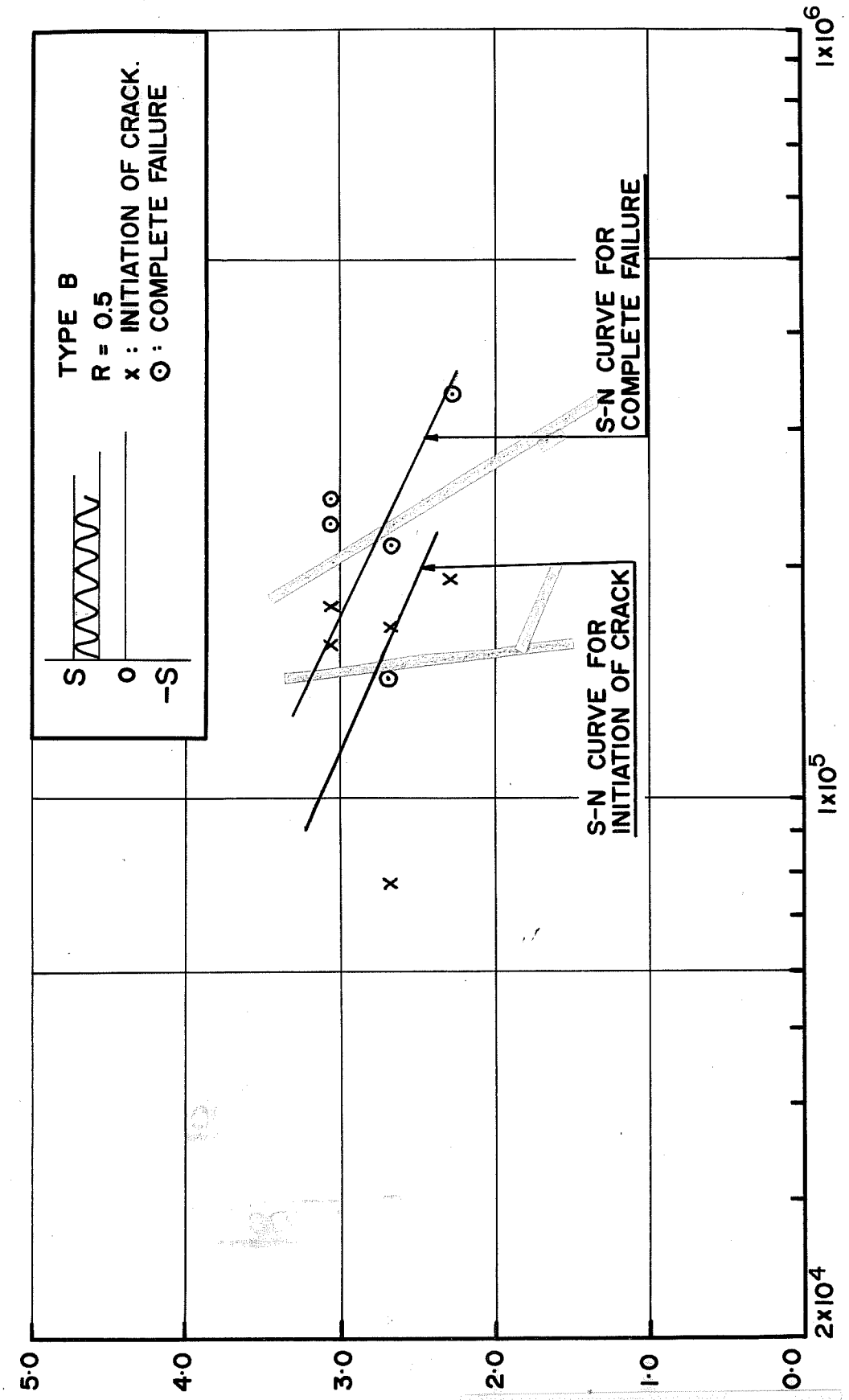

FIG. 21 S-N DIAGRAM FOR TYPE B SPECIMENS

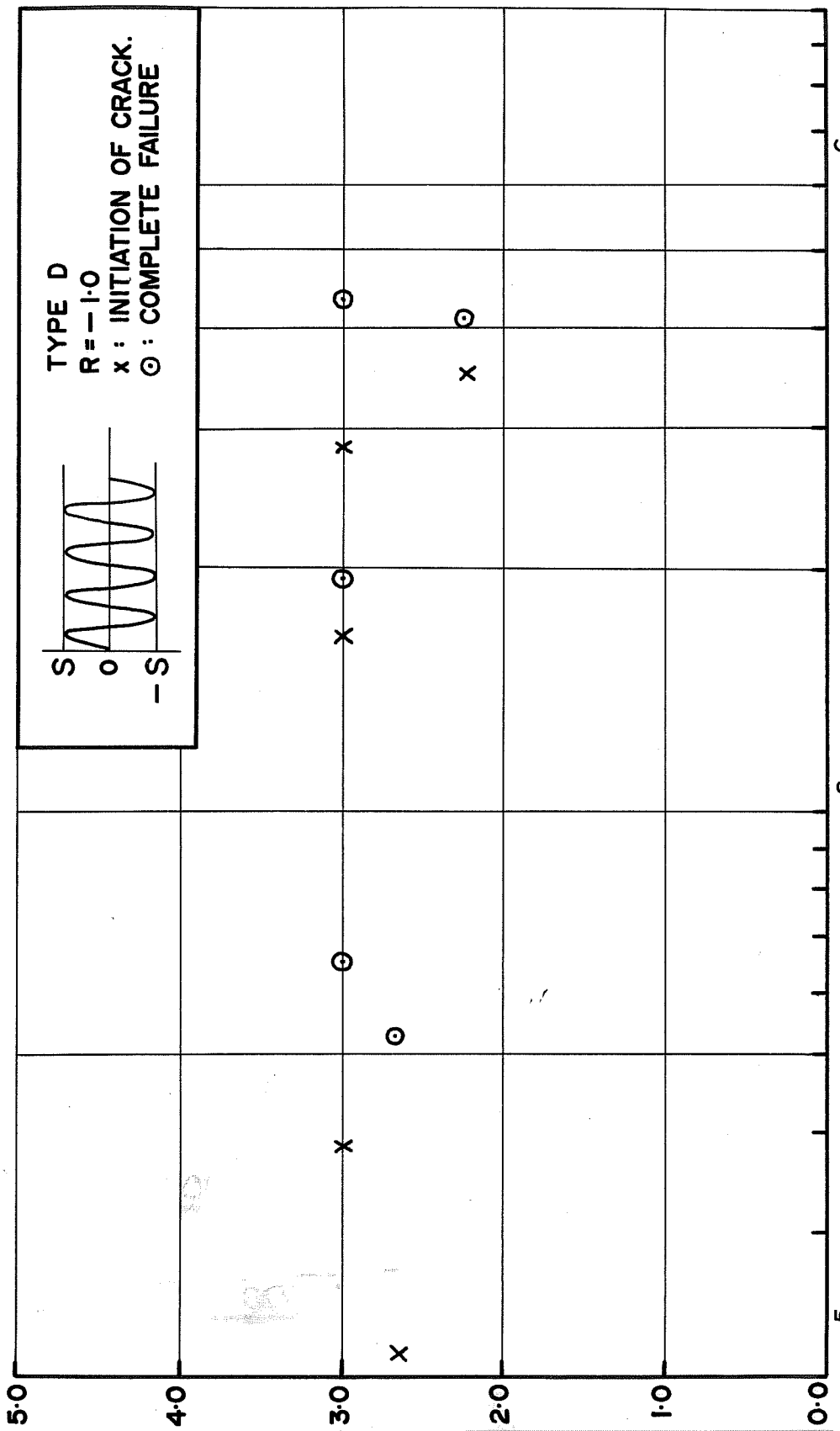

FIG.23 S–N DIAGRAM FOR TYPE D SPECIMENS

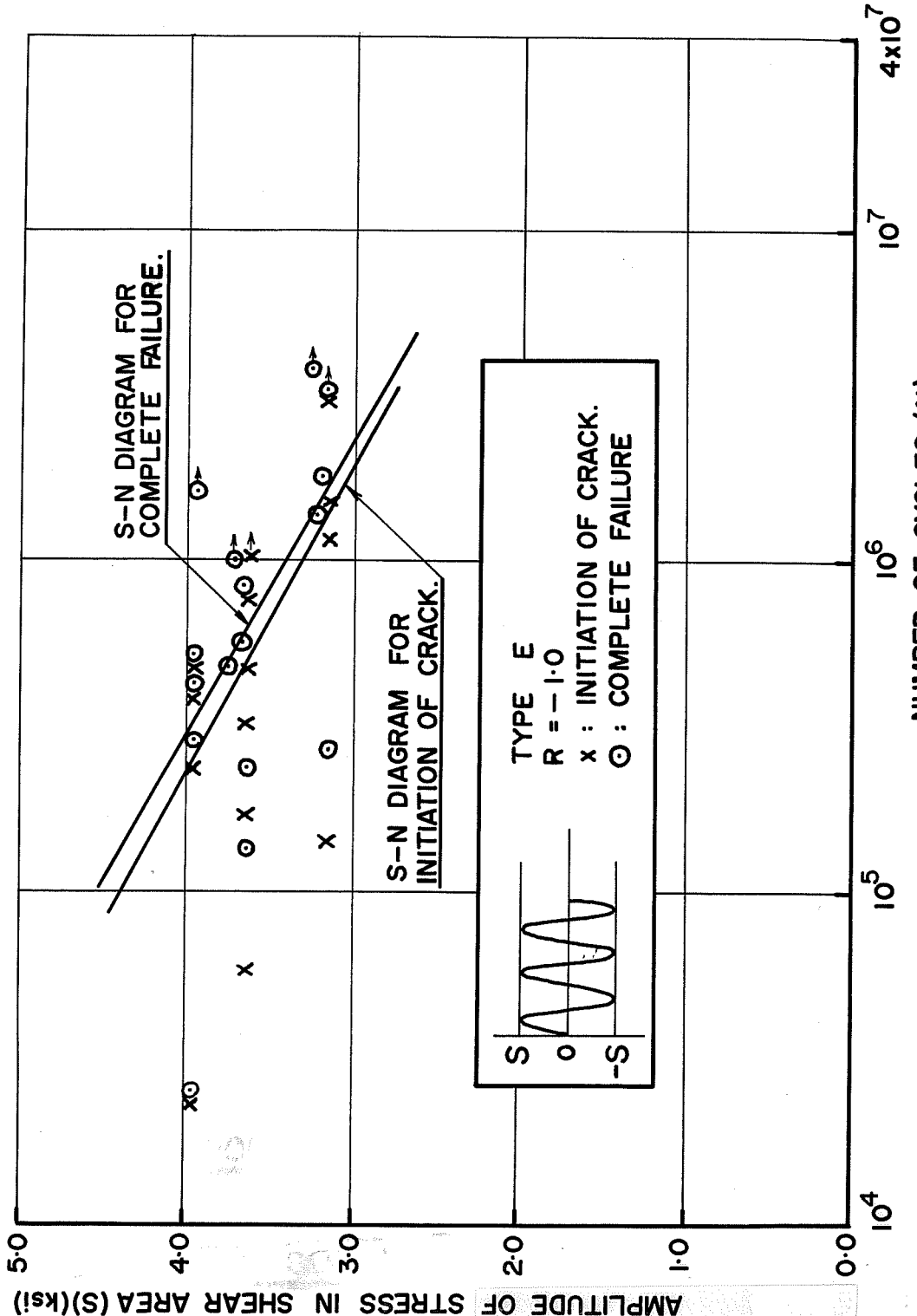

FIG. 24 S-N DIAGRAM FOR TYPE E SPECIMENS

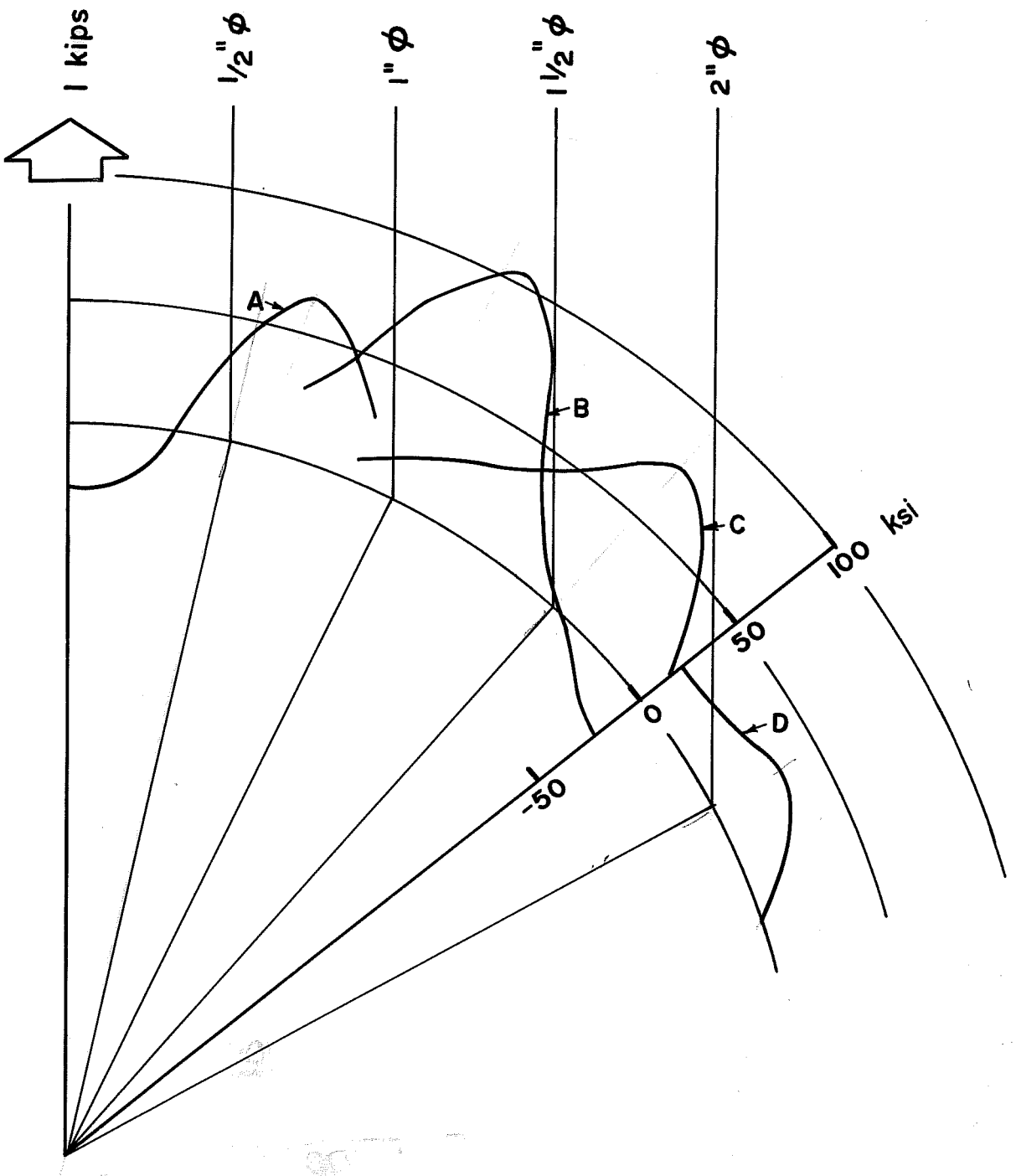

FIG.25 CIRCUMFERENTIAL STRESS ACCORDING TO ELASTIC THEORY

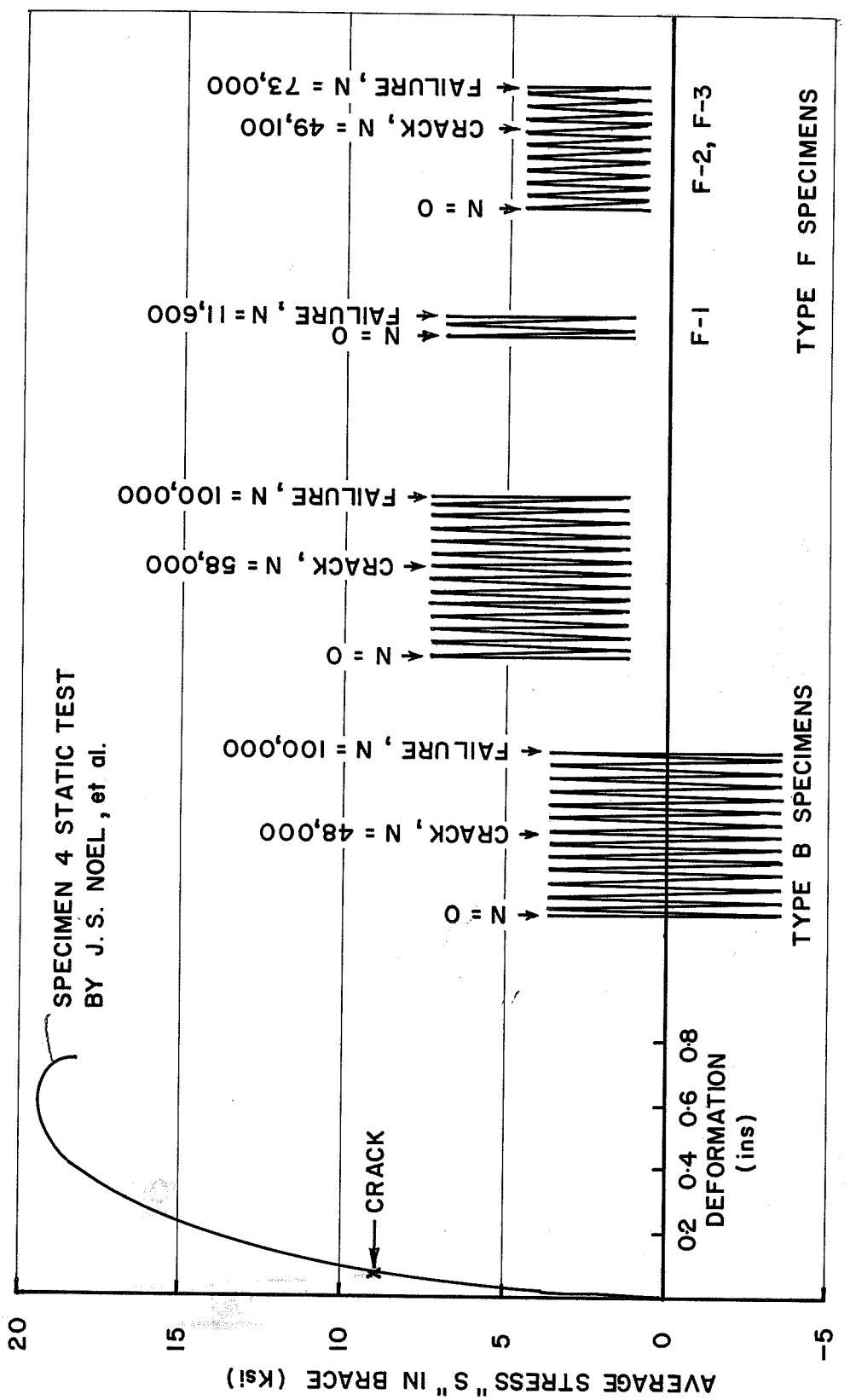

FIG.28 COMPARISON BETWEEN STATIC TEST AND FATIGUE TESTS.

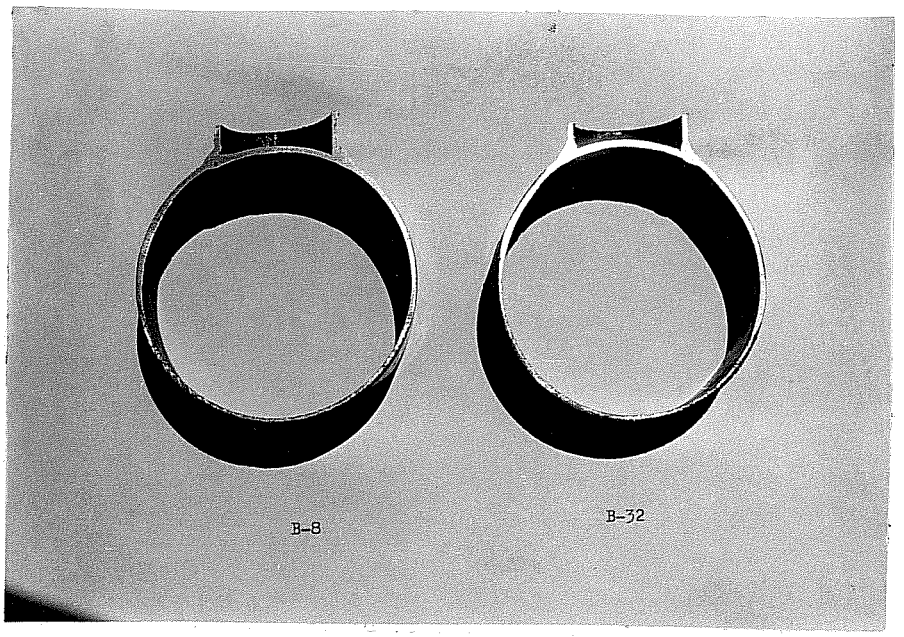

Fig. 29 a Cross Section of Specimen Type B

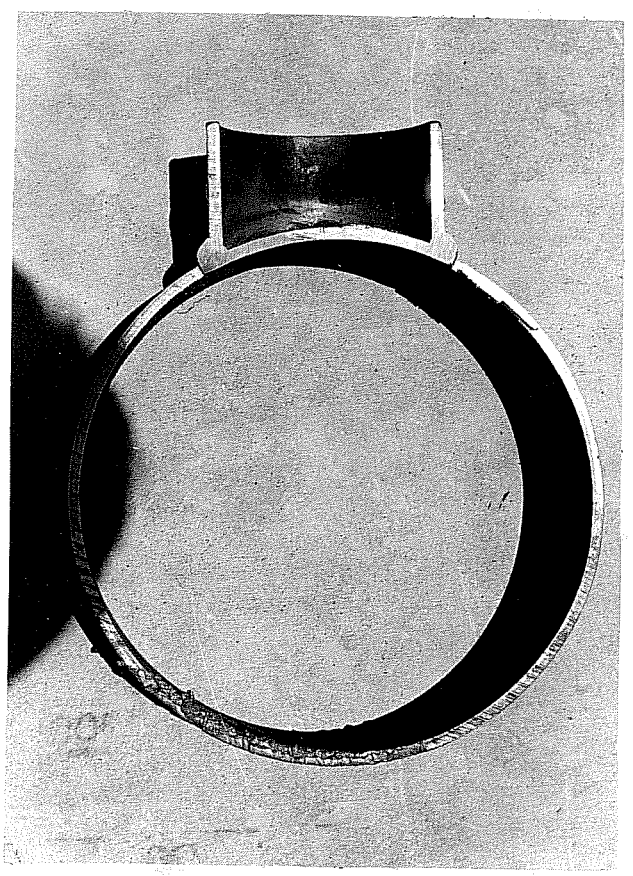

Fig. 29 b Cross Section of Specimen Type F